iScience

CellPress

Article

Antagonistic Glucagon Receptor Antibody Promotes α-Cell Proliferation and Increases β-Cell Mass in Diabetic Mice

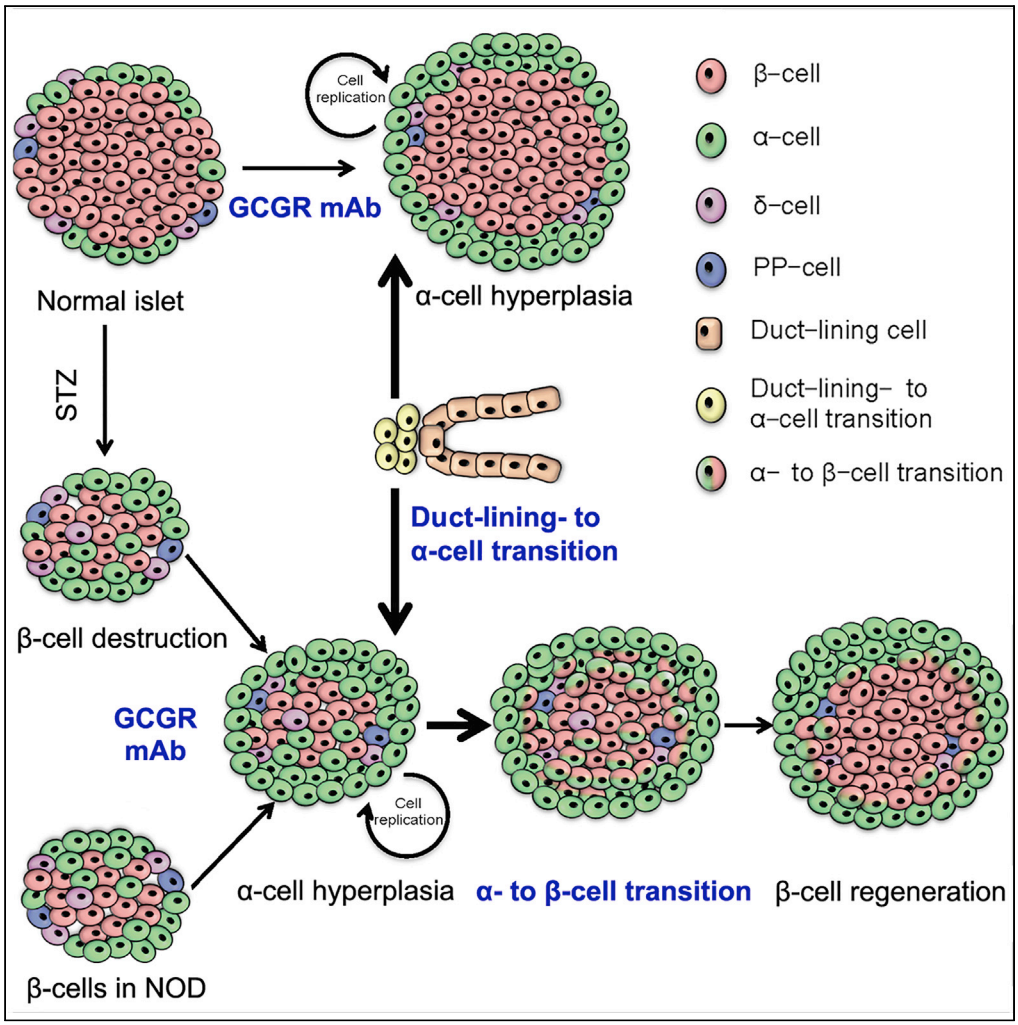

Rui Wei, Liangbiao Gu, Jin Yang, ..., Dung Thai, Hai Yan, Tianpei Hong

tpho66@bjmu.edu.cn

HIGHLIGHTS

GCGR mAb induced α-cell expansion by neogenesis and cell proliferation

GCGR mAb increased the β-cell mass in type 1 diabetic mice

GCGR mAb might promote α- to β-cell conversion in type 1 diabetic mice

Wei et al., iScience 16, 326–339
June 28, 2019
https://doi.org/10.1016/j.isci.2019.05.030

iScience

CellPress

Article

Antagonistic Glucagon Receptor Antibody Promotes α-Cell Proliferation and Increases β-Cell Mass in Diabetic Mice

Rui Wei,[1,2,5] Liangbiao Gu,[1,2,5] Jin Yang,[1,2] Kun Yang,[1] Junling Liu,[1,2] Yunyi Le,[1] Shan Lang,[1,2] Haining Wang,[1] Dung Thai,[3,4] Hai Yan,[3,4] and Tianpei Hong[1,2,6,*]

SUMMARY

Under extreme conditions or by genetic modification, pancreatic α-cells can regenerate and be converted into β-cells. This regeneration holds substantial promise for cell replacement therapy in diabetic patients. The discovery of clinical therapeutic strategies to promote β-cell regeneration is crucial for translating these findings into clinical applications. In this study, we reported that treatment with REMD 2.59, a human glucagon receptor (GCGR) monoclonal antibody (mAb), lowered blood glucose without inducing hypoglycemia in normoglycemic, streptozotocin-induced type 1 diabetic (T1D) and non-obesity diabetic mice. Moreover, GCGR mAb treatment increased the plasma glucagon and active glucagon-like peptide-1 levels, induced pancreatic ductal ontogenic α-cell neogenesis, and promoted α-cell proliferation. Strikingly, the treatment also increased the β-cell mass in these two T1D models. Using α-cell lineage-tracing mice, we found that the neogenic β-cells were likely derived from α-cell conversion. Therefore, GCGR mAb-induced α- to β-cell conversion might represent a pre-clinical approach for improving diabetes therapy.

INTRODUCTION

Diabetes is increasing in prevalence worldwide, particularly in rapidly developing countries, such as China, which currently has the world's largest diabetes epidemic (Wang et al., 2017). Type 1 diabetes (T1D) or type 2 diabetes (T2D) ultimately results in pancreatic β-cell loss and chronic hyperglycemia. The replacement of lost β-cells using various approaches, such as pancreatic or islet transplantation, stem cell differentiation, and mature somatic cell reprogramming, represents a promising therapeutic strategy (Vieira et al., 2016). Pancreatic α- and β-cells have similar epigenetic landscapes (Bramswig et al., 2013), express many of the same transcription factors (e.g., Pax6 and Isl1), and metabolize glucose and secrete hormones via similar mechanisms (e.g., glucokinase and ATP-sensitive K^+ channel). These similarities make reprogramming α-cells into β-cells easier than other types of cell conversion. α- and β-cells are situated within the islets and are both close to the vasculature (Bosco et al., 2010), which suggests that α-cells are well positioned for ideal β-cell function (Thorel et al., 2011). Moreover, a small amount of glucagon remaining after α-cell ablation is sufficient to maintain the metabolic effects of glucagon (Thorel et al., 2011). Notably, under diverse conditions of β-cell injuries in animals and humans, the α-cell mass is preserved or increased (Marroqui et al., 2015), which constitutes a potentially abundant source for reprogramming. Thus, endogenous α-cells are an attractive source for β-cell regeneration (Wei and Hong, 2016). Under certain extreme conditions (e.g., diphtheria toxin-induced β-cell ablation >99% or combination of pancreatic duct ligation with alloxan), α-cells can spontaneously transdifferentiate into β-cells (Chung et al., 2010; Thorel et al., 2010). Forced expression of *Pax4* (a master regulator of the β-cell lineage) or selective inhibition of *Arx* (a master regulator of the α-cell lineage) in α-cells can promote α- to β-cell conversion in adult mice of any age (Collombat et al., 2009; Al-Hasani et al., 2013; Courtney et al., 2013). However, these extreme conditions or transgenic approaches cannot be directly translated into diabetes therapy in humans. Recently, γ-aminobutyric acid and artemisinin (an anti-malarial drug) were identified as chemical inducers of α-to β-cell conversion (Ben-Othman et al., 2017; Li et al., 2017). Nevertheless, the effect of small molecules remains to be further clarified (van der Meulen et al., 2018), and the safety of their long-term treatment must be determined in humans. It is highly desirable and valuable to investigate and validate the pro-β-cell neogenic effects of drug candidates that are in both pre-clinical and clinical stages.

In addition to pancreatic β-cells and insulin, the effects of α-cells and glucagon on glucose homeostasis regulation and diabetes development have long been recognized and have become increasingly

[1]Department of Endocrinology and Metabolism, Peking University Third Hospital, Beijing 100191, China

[2]Clinical Stem Cell Research Center, Peking University Third Hospital, Beijing 100191, China

[3]REMD Biotherapeutics, Camarillo, CA 93012, USA

[4]Beijing Cosci-REMD, Beijing 102206, China

[5]These authors contributed equally

[6]Lead Contact

*Correspondence: tpho66@bjmu.edu.cn

https://doi.org/10.1016/j.isci.2019.05.030

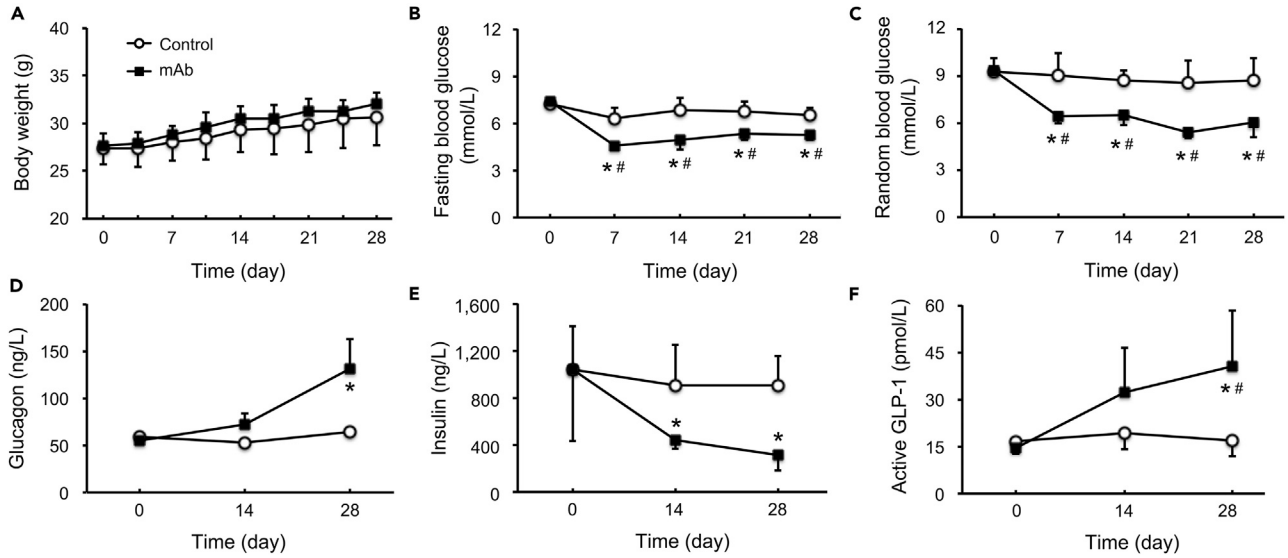

Figure 1. Metabolic Parameters in Normal Male C57BL/6N Mice Treated With REMD 2.59, a Human Glucagon Receptor (GCGR) Monoclonal Antibody (mAb), or Saline (as Control) for 4 Weeks

(A) Body weight; (B) fasting blood glucose; (C) random blood glucose; (D) plasma glucagon; (E) plasma insulin; (F) plasma active glucagon-like peptide-1 (GLP-1). n = 6–10 mice per group. Data are expressed as the mean ± S.D. Statistical analysis was conducted by Student's t test. *$p < 0.05$ (GCGR mAb vs. control); $^{\#}p < 0.05$ (posttreatment vs. pretreatment in the same group).

emphasized (Unger and Orci, 1977). Blockage of the glucagon receptor (GCGR) by gene knockout, antisense oligonucleotides, or specific antagonists improves hyperglycemia and other metabolic manifestations of insulin deficiency in diabetic subjects (Sloop et al., 2004; Lee et al., 2012; Lotfy et al., 2014). REMD 2.59, a fully competitive antagonistic human GCGR monoclonal antibody (mAb), and REMD-477, another human GCGR mAb that differs by only one amino acid (which is not involved in glucagon binding) and has an affinity for the GCGR equivalent to that of REMD 2.59, have shown strong hypoglycemic effects in T1D rodents (Wang et al., 2015), T2D rodents, and non-human primates (Yan et al., 2009; Okamoto et al., 2015), as well as patients with T1D (Pettus et al., 2018). Notably, blockage of the GCGR in animals resulted in α-cell hyperplasia (Sloop et al., 2004; Lee et al., 2012; Okamoto et al., 2015). Strikingly, in mice with diphtheria-toxin-induced extreme β-cell loss, *Gcgr* knockout increased glucagon-insulin co-expressing cells (Damond et al., 2016). Moreover, in mice with insulin receptor antagonist-induced severe insulin resistance, GCGR mAb not only expanded the α-cell mass but also increased the β-cell mass (Okamoto et al., 2017). However, despite these observations, whether the GCGR mAb enlarges the β-cell mass via promoting α- to β-cell conversion in normal and stressed conditions remains to be clarified.

In the present study, we showed that treatment with an antagonistic GCGR mAb induced pancreatic duct-derived α-cell neogenesis, promoted α-cell proliferation, and increased the islet number and area in normoglycemic, streptozotocin (STZ)-induced T1D and non-obesity diabetic (NOD) mice. Moreover, GCGR mAb treatment expanded the β-cell mass likely via α- to β-cell conversion in these two T1D models. Our findings suggest that treatment with the GCGR mAb might be a pre-clinical path for pancreatic β-cell regeneration in diabetes.

RESULTS

GCGR mAb Lowers Blood Glucose and Increases Plasma Glucagon and Active Glucagon-like Peptide-1 Levels in Normal C57BL/6N Mice

Normal male C57BL/6N mice were treated with REMD 2.59, a human GCGR mAb and competitive antagonist, to evaluate its metabolic effects. During the 4-week treatment, no significant difference was identified between the GCGR mAb and control groups in terms of body weight ($p = 0.36$) (Figure 1A). A single injection of the GCGR mAb significantly lowered the fasting and random blood glucose levels (both $p < 0.001$). The glycemic levels were lower in the GCGR mAb group than in the control group during the 4 weeks of treatment and were within the normal range with little fluctuation (Figures 1B and 1C). Weekly administration of the GCGR mAb for 4 weeks significantly increased the plasma glucagon levels compared with those in the control group (131.6 ± 31.0 ng/L

vs. 64.7 ± 4.3 ng/L, p = 0.039) (Figure 1D). Notably, the plasma insulin level was decreased (p = 0.004) (Figure 1E), whereas active glucagon-like peptide-1 (GLP-1) level was increased (p = 0.019) (Figure 1F), by the GCGR mAb treatment in the normoglycemic mice.

GCGR mAb Induces Pancreatic Duct-Derived α-Cell Neogenesis, Promotes α-Cell Proliferation, and Increases the α-Cell Mass in Normal C57BL/6N Mice

Histological analysis of pancreatic islets was performed using immunofluorescence staining. Treatment with the GCGR mAb induced a massive expansion in the number of glucagon-positive α-cells (48 [32, 91] vs. 19 [8, 36] per islet slice, p < 0.001) (Figures 2A and 2B). Notably, the glucagon-positive α-cells were located not only in the islet mantle zone but also in the islet core, where insulin-positive β-cells are generally detected. The number of insulin-positive β-cells remained unchanged following GCGR mAb treatment (p = 0.42), thereby decreasing the proportion of β-cell numbers to α-cell numbers (p < 0.001) (Figures 2A and 2B). Moreover, we also found that the islet number (p < 0.001) and area (p = 0.001) were significantly increased by GCGR mAb treatment (Figures S1A–S1C). Interestingly, the insulin labeling intensity, as shown by immunofluorescence staining, was weaker in the GCGR mAb group than in the control group. In contrast to the typical observation that insulin staining is generally located throughout the entire cytoplasm of β-cells, insulin labeling was mainly detected in the cytoplasm around the nucleus and was barely detectable in other parts of the cytoplasm after GCGR mAb treatment (Figure 2A).

We subsequently estimated the possible origin of the expanded pancreatic α-cells. We noted that the positioning of these α-cells within the islets was atypical, as most cells were detected in cell clusters close to pancreatic ducts but were not uniformly distributed within the islet mantle zone, as exhibited in the controls. Interestingly, some glucagon-positive α-cells were also detected in the ductal region (Figure 2C). These findings suggest that these neogenic α-cells might have derived from ducts. We subsequently carried out double-immunostaining using specific antibodies for glucagon and cytokeratin 19 (CK19), a marker of mature duct cells. Again, some glucagon-positive α-cells were located in the duct compartment (Figure 2D). However, we did not identify the co-localization of glucagon with CK19, which indicates that these neogenic α-cells might not have directly derived from mature duct cells. Moreover, we performed additional double-labeling studies using two other ductal cell markers (Hnf1β and Sox9) to further strengthen our findings of duct- to α-cell neogenesis. Similarly, we found that some glucagon-positive α-cells were located in the duct lining (Figure S2A). Surprisingly, we also found that a few cells were Hnf1β and glucagon double-positive (Figure S2A). We did not find any α-cells located in ducts in the control group. Because Hnf1β and Sox9 are also expressed in the pancreatic progenitors, we inferred that the neogenic α-cells might be differentiated from the progenitors located in ducts. Except for neogenesis, we also performed immunostaining of proliferating cell nuclear antigen (PCNA) to detect cell proliferation. We found that the numbers of glucagon and PCNA double-positive cells were almost doubled by mAb treatment (1.86 ± 0.53% vs. 0.92 ± 0.37%, p = 0.001) (Figure S3A), which suggested neogenic α-cells could also be derived from self-replication.

GCGR mAb Decreases Blood Glucose and Increases Plasma Glucagon, Insulin, and Active GLP-1 Levels in STZ-Induced Diabetic Mice

To investigate the effects of the GCGR mAb on diabetic mice, we used STZ to establish a T1D model in male C57BL/6N mice. During the 4 weeks of treatment, there was no significant difference in the body weights between the GCGR mAb and control groups in the STZ-induced T1D mice (p = 0.36) (Figure 3A). A single injection of the GCGR mAb significantly lowered the fasting and random blood glucose levels (both p < 0.001), and the lowering effects maintained throughout the entire study period (Figures 3B and 3C). The GCGR mAb treatment significantly increased the plasma glucagon levels, and the increase was more pronounced after the 4-week treatment (1,261.1 ± 290.6 ng/L vs. 80.2 ± 15.1 ng/L, p = 0.005) (Figure 3D). Notably, the plasma insulin (p = 0.024), C-peptide (p < 0.001), and active GLP-1 (p = 0.005) levels were substantially higher after treatment with the GCGR mAb (Figures 3E, 3F, and S4A).

GCGR mAb Induces Pancreatic Duct-Derived α-Cell Neogenesis, Promotes α-Cell Proliferation, and Increases the α-Cell Mass in STZ-Induced Diabetic Mice

Histological analysis of the pancreatic islets was carried out using immunofluorescence staining in STZ-induced T1D mice. Similar to the findings in the normal C57BL/6N mice, the GCGR mAb treatment strongly augmented the number of glucagon-positive α-cells (68 [35, 139] vs. 53 [35, 73] per islet slice, p = 0.035), and the glucagon-positive α-cells were located not only in the islet mantle zone but also in the islet core (Figures 4A and 4B). Strikingly, the number of insulin-positive β-cells significantly increased (17 [8, 30] vs. 5 [3, 8] per

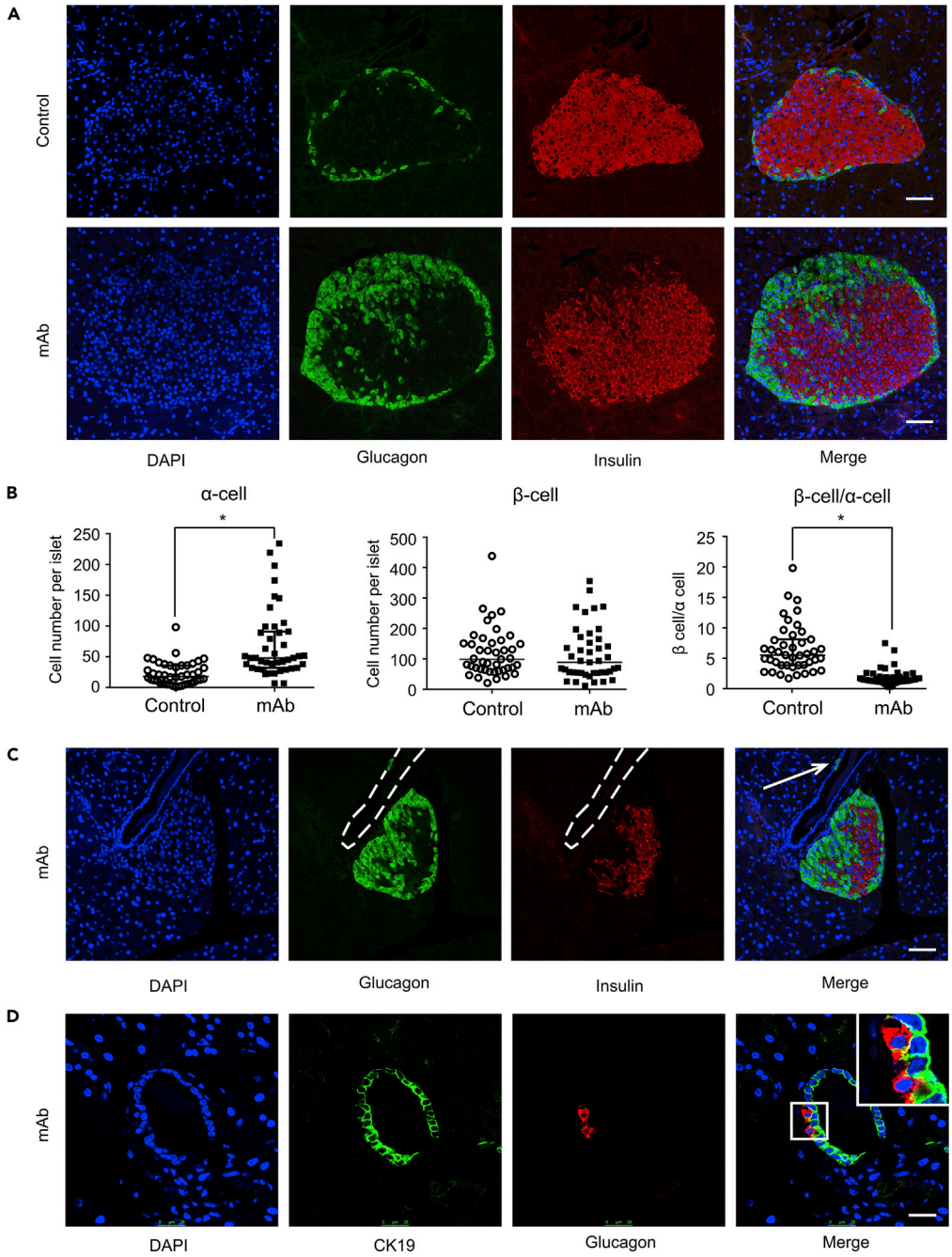

Figure 2. Histological Analysis in the Pancreata of Normal Male C57BL/6N Mice Treated with the GCGR mAb or Saline Control for 4 Weeks

(A) Representative image of an islet immunostained for glucagon and insulin.

(B) Quantification of α-cells and β-cells per islet slice and the proportion of β-cell numbers to α-cell numbers. n = 5–8 sections/mouse multiplied by 6–9 mice/group. Data are expressed as the median (interquartile range). Statistical analysis was conducted by the Mann-Whitney test. *$p < 0.05$ (GCGR mAb vs. control).

(C) Representative photograph showing glucagon-positive cells located in the ductal region. The ductal lumen is outlined with dashed lines. The arrow indicates glucagon-positive cells in the ductal lining.

(D) Representative image of co-labeling for glucagon and cytokeratin 19 (CK19), a marker of mature duct cells. The cells in the small box are enlarged at the top-right corner of the image.

Scale bar, 100 μm. See also Figures S1A–S1C, S2A, and S3A.

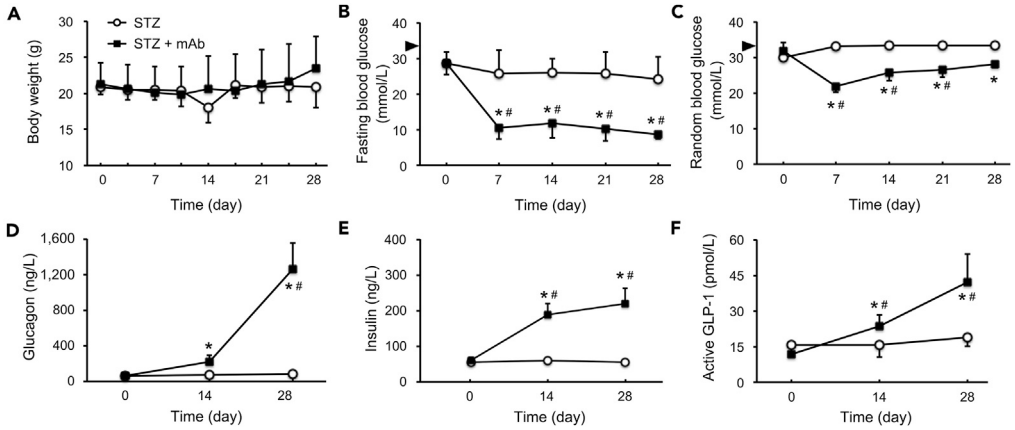

Figure 3. Metabolic Parameters in Streptozocin (STZ)-Induced Type 1 Diabetic (T1D) Male C57BL/6N Mice Treated with the GCGR mAb or Saline Control for 4 Weeks

(A) Body weight; (B) fasting blood glucose; (C) random blood glucose; (D) plasma glucagon; (E) plasma insulin; (F) plasma active GLP-1. n = 6–10 mice per group. Data are expressed as the mean ± S.D. Statistical analysis was conducted by Student's t test. *$p < 0.05$ (GCGR mAb vs. Saline); $^{\#}p < 0.05$ (posttreatment vs. pretreatment in the same group). The arrowheads in (B and C) indicate the upper detection limit of the glucometer (33.3 mmol/L).

See also Figure S4A.

islet slice, $p < 0.001$), and the proportion of β-cell numbers to α-cell numbers substantially increased (0.18 [0.12, 0.39] vs. 0.11 [0.05, 0.16], $p < 0.001$) following GCGR mAb treatment compared with the saline control (Figures 4A and 4B). Again, the islet number and area per pancreatic section were significantly increased by the GCGR mAb treatment (Figure S1D).

We subsequently explored the possible source of the regenerated α-cells. Similar to the findings in the normal C57BL/6N mice, some glucagon-positive α-cells were found in the ductal region (Figure 4C) in the GCGR mAb-treated diabetic mice, whereas in the saline group not. We inferred that these neogenic α-cells in the GCGR mAb-treated T1D mice might also have originated from ducts. We carried out double immunostaining of glucagon with duct cell markers, including CK19, Sox9, and Hnf1β. Again, some glucagon-positive α-cells were located in the duct compartment (Figures 4D and S2B). Although there was no co-localization of glucagon with CK19, some cells were double positive for glucagon with Sox9 or Hnf1β (Figures 4D and S2B), which indicates that these neogenic α-cells might not have directly derived from mature duct cells; instead, they may have differentiated from the progenitors located in ducts. Besides, we performed PCNA staining to detect cell proliferation. We found that the numbers of glucagon and PCNA double-positive cells were upregulated by STZ treatment (1.28 ± 0.35% vs. 0.92 ± 0.37%, $p = 0.028$) and were further boosted by the GCGR mAb treatment (2.76 ± 0.80% vs. 1.28 ± 0.35%, $p = 0.002$) (Figure S3A), which suggested neogenic α-cells could also be derived from self-replication. Interestingly, we also noted that several PCNA positive cells were located in the duct (Figure S3A), suggesting mAb might promote duct cell or duct progenitor proliferation.

Pancreatic β-Cell Mass Increases and Neogenic β-Cells Are Likely Derived from α-Cell Conversion in GCGR mAb-Treated STZ-Induced Diabetic Mice

The β-cell mass was enlarged in the pancreata of the GCGR mAb-treated T1D mice (Figures 4A and 4B). To determine the source of the hyperplastic β-cells, further immunofluorescence analyses were performed. The vast majority of the newly formed insulin-positive β-cells were found in the islet core (Figure 4A), and in some cases, insulin-positive β-cells were located in the islet mantle zone (Figure 4C), where glucagon-positive α-cells are classically detected. Notably, we did not identify insulin-positive β-cells in the ductal region, which suggests that β-cells might not have directly derived from the duct lining. In some cases, we observed cells co-expressing both glucagon and insulin (Figure 4A), which indicates that α-cells might have been the origin of β-cells in the GCGR mAb-treated diabetic mice. We also found that some glucagon-positive cells co-immunostained with Pdx1 (a key transcription factor for β-cell maturation and function), Nkx6.1 (another transcription factor for β-cell development and function), or prohormone convertase 1/3 (PC1/3, an important enzyme for proinsulin processing in β-cells) (Figures 5A–5C).

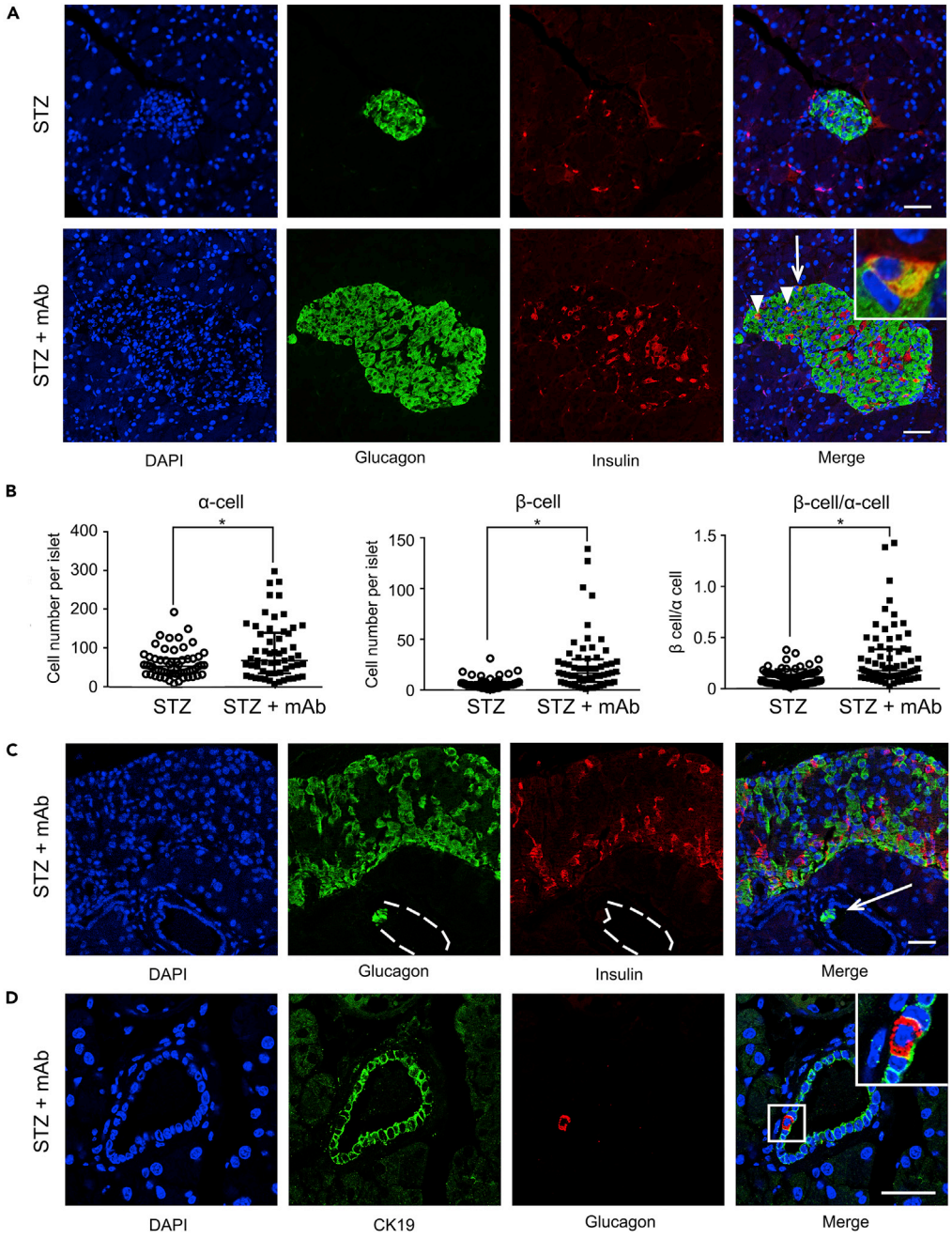

Figure 4. Histological Analysis in the Pancreata of STZ-Induced T1D Male C57BL/6N Mice Treated with the GCGR mAb or Saline Control for 4 Weeks

(A) Representative image of an islet immunostained for glucagon and insulin. The arrows and arrowheads indicate co-labeling, and the co-labeled cells indicated by the arrows are enlarged at the top-right corner of the image.

(B) Quantification of α-cells and β-cells per islet slice and the proportion of β-cell numbers to α-cell numbers. n = 6–9 sections/mouse multiplied by 8 mice/group. Data are expressed as the median (interquartile range). Statistical analysis was conducted by the Mann-Whitney test. *$p < 0.05$ (GCGR mAb vs. Saline).

(C) Representative photograph showing glucagon-positive cells located in the ductal region. The ductal lumen is outlined with dashed lines. The arrow indicates glucagon-positive cells in the ductal lining.

(D) Representative image of co-immunostaining with glucagon and cytokeratin 19 (CK19). The cells in the small box are enlarged at the top-right corner of the image.

Scale bar, 100 μm. See also Figures S1D, S2B, and S3B.

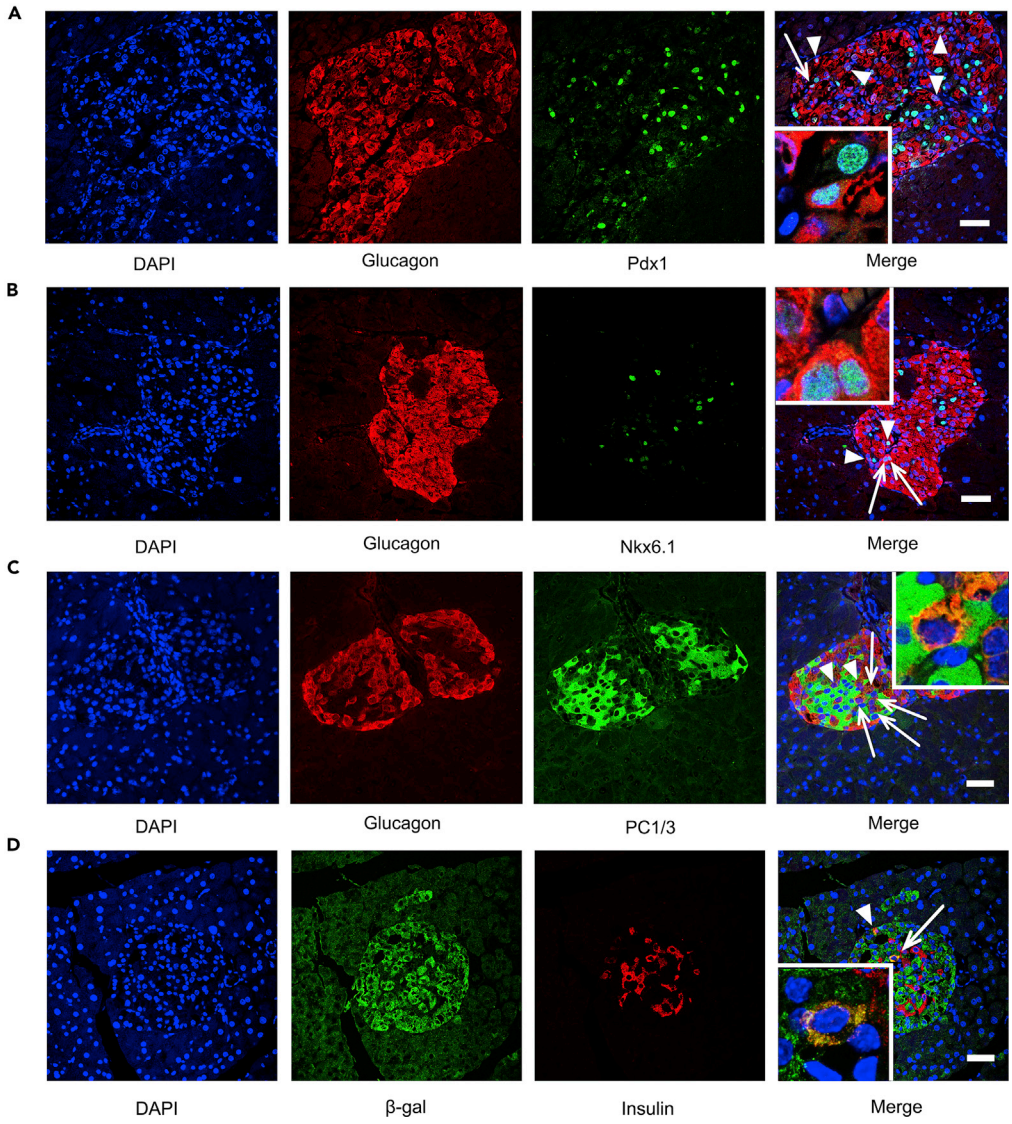

Figure 5. Immunofluorescence Analysis of Pancreatic α- to β-Cell Conversion in STZ-Induced T1D Mice Treated with the GCGR mAb

(A) Representative photograph of an islet immunolabeled with glucagon and Pdx1, a master transcription factor that participates in pancreatic fate determination and β-cell maturation and function, in STZ-induced T1D C57BL/6N mice treated with the GCGR mAb for 4 weeks.

(B) Representative photograph of an islet immunolabeled with glucagon and Nkx6.1, a transcription factor involved in β-cell development and function, in the same animals as (A).

(C) Representative photograph of an islet immunolabeled with glucagon and prohormone convertase 1 (PC1/3), an enzyme essential for proinsulin processing in β-cells, in the same animals as (A).

(D) Representative image of an islet immunostained with β-gal and insulin in STZ-induced T1D *glucagon-β-gal* mice treated with the GCGR mAb for 8 weeks.

The arrows and arrowheads indicate co-labeling, and the co-labeled cells indicated by the arrows are enlarged at the corners of the images. Scale bar, 100 μm. See also Figures S5 and S6.

To confirm the α- to β-cell conversion, we used pancreatic α-cell lineage-tracing *glucagon-β-gal* mice. The T1D model in these mice was also induced by STZ, and the mice were treated with GCGR mAb or saline. The body weights, the fasting and random blood glucose levels, the plasma glucagon, insulin and active GLP-1 levels showed similar changes to the non-tracing mice (Figure S5). The immunostaining showed that most of the glucagon-positive cells were labeled with β-gal (Figure S6), suggestive of a

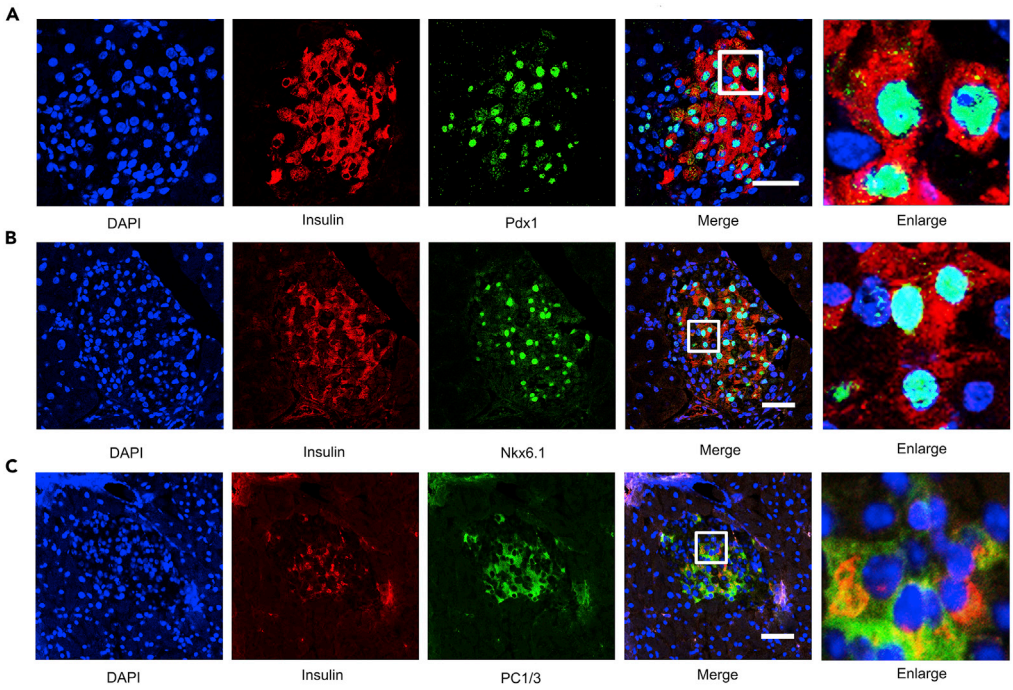

Figure 6. Immunofluorescence Analysis of β-Cell Markers in the Pancreata of STZ-Induced T1D Mice Treated with the GCGR mAb for 4 Weeks

(A) Representative image of an islet immunostained with insulin and Pdx1.

(B) Representative photograph of an islet immunolabeled with insulin and Nkx6.1.

(C) Representative image of an islet immunostained with insulin and PC1/3.

The cells in the boxes are enlarged in the fifth columns. Scale bar, 100 μm.

high lineage-tracing efficiency. Importantly, we not only observed glucagon and insulin double-positive cells (Figure S6) but also found that some insulin-positive cells contained α-cell labeled β-gal in the pancreata of the GCGR mAb group (Figures 5D and S6). These results provided strong evidence that treatment with the GCGR mAb contributed to the conversion of glucagon-expressing α-cells into insulin-positive β-cells in STZ-induced T1D mice.

Next, we detected whether the GCGR mAb treatment promoted β-cell proliferation. We performed PCNA immunostaining and found that the proportion of C-peptide and PCNA double-positive cells was only slightly upregulated by the GCGR mAb in T1D mice (2.17 ± 0.75% vs. 1.37 ± 0.54%, $p = 0.08$) (Figure S3B), suggesting self-replication may not be a key contributing factor for the increased β-cell mass.

Neogenic β-cells in GCGR mAb-Treated STZ-Induced Diabetic Mice Appear to Be Mature Pancreatic β-Cells

To further characterize the newly formed insulin-positive β-cells in the pancreata of GCGR mAb-treated T1D mice, we performed double immunostaining of insulin with one of several other specific markers for β-cells. Most insulin-positive cells in the islets of the GCGR mAb-treated diabetic mice co-expressed with bona fide β-cell markers, including the transcription factors Pdx1 (Figure 6A) and Nkx6.1 (Figure 6B), as well as the proinsulin-processing enzyme PC1/3 (Figure 6C). These results indicated that the newborn insulin-positive β-cells had the molecular machinery required for functional maturation.

GCGR mAb Decreases Blood Glucose and Increases Plasma Glucagon and Insulin Levels in Diabetic NOD Mice

T1D is characterized not only by the massive loss of β-cells but also an autoimmune insulitis in which autoreactive T-cells are activated. The NOD mouse is a classical tool of autoimmune diabetes. Therefore, we investigated whether GCGR mAb treatment could lower blood glucose, induce α-cell neogenesis,

promote α-cell proliferation, and initiate α- to β-cell conversion in diabetic NOD mice. During the 4 weeks of treatment, the body weights in the control group displayed a slight but steady decrease ($p = 0.05$); in contrast, in the GCGR mAb group, the body weights remained unchanged ($p = 0.505$). At the end of the treatment, the body weights in the GCGR mAb group were higher than those in the control group ($p < 0.001$) (Figure 7A). A single injection of the GCGR mAb significantly lowered the fasting blood glucose levels ($p < 0.001$). The glycemic levels were lower in the GCGR mAb group than in the control group throughout the entire study period (all $p < 0.001$, Figure 7B). Administration of the GCGR mAb significantly increased the plasma glucagon levels compared with the saline control (2,020.5 ± 1,207.6 ng/L vs. 111.0 ± 54.3 ng/L, $p = 0.029$) (Figure 7C). Similar to the findings in the STZ-induced T1D mice, the plasma insulin ($p = 0.049$) and C-peptide ($p = 0.023$) levels were significantly increased, and the active GLP-1 level was slightly upregulated ($p = 0.075$) by treatment with the GCGR mAb in the NOD mice (Figures 7D, S4B, and S7A).

GCGR mAb Promotes Pancreatic Duct-Derived α-Cell Neogenesis and Increases the α- and β-Cell Mass in Diabetic NOD Mice

Immunofluorescence staining in the pancreata of diabetic NOD mice was performed. We found that, with the exception of the glucagon-positive α-cells and residual insulin-positive β-cells, a large number of infiltrative cells surrounded the islets (Figure 7E), which was the classical lymphocytic infiltration as previously reported (Brode et al., 2006). Similar to the findings in the normal C57BL/6N and STZ-induced diabetic mice, the GCGR mAb treatment augmented the number of α-cells (29 [17, 51] vs. 18 [11, 26] per islet slice, $p < 0.001$) (Figures 7E and S7B), and the glucagon-positive α-cells were located not only in the islet mantle zone but also in the islet core (Figure 7E). The islet structure remained intact, and the number of insulin-positive β-cells was higher in the GCGR mAb treatment group than in the control group in NOD mice (26 [6, 56] vs. 4 [1, 27] per islet slice, $p < 0.001$) (Figures 7E and S7C). We subsequently explored the cell origin of α-cells. Results showed that α-cell clusters were close to pancreatic ducts (Figure 7F), and some glucagon-positive cells were located in the ductal region (Figure 7G) in the GCGR mAb-treated NOD mice, which suggests that these neogenic α-cells might have originated from ducts. We also found glucagon and insulin bihormonal cells (Figures 7E and 7F), suggestive of α- to β-cell conversion. Notably, most of the bihormonal cells were detected in the neogenic islets. These islets were close to pancreatic ducts and were predominantly composed of α-cells with little or no insulitis (Figure 7F). These results suggested that the newborn α-cells and bihormonal cells might be resistant to autoimmune reaction.

DISCUSSION

We report an unexpected effect of REMD 2.59, a human GCGR mAb, on inducing the conversion of pancreatic α-cells into β-cells in two T1D mouse models. GCGR mAb treatment seemed to mobilize ductal progenitors to generate α-cells and promote α-cell proliferation, which resulted in increased islet number and area. Pancreatic α-cells were subsequently reprogrammed into β-cells under the diabetic environment. Moreover, the regenerated β-cells expressed markers specific for functional mature β-cells. Therefore, these findings could pave the way for therapies to restore the β-cell mass in diabetic patients.

Long ignored or neglected, pancreatic α-cells, which co-inhabit islets with β-cells, have recently captured attention because of breakthrough findings highlighting the importance of these cells in the maintenance of β-cell functions and glucose homeostasis (Lee et al., 2016). Glucagon, secreted from α-cells, appears to be a major factor in the pathophysiology of diabetes (Kulina and Rayfield, 2016). Inhibiting glucagon secretion or antagonizing its action is currently considered an innovative approach to diabetes treatment. Several anti-diabetic drugs currently used to treat patients with T2D may partially exert their hypoglycemic effects via reducing glucagon secretion (e.g., GLP-1 receptor agonists, dipeptidyl peptidase-4 inhibitors) or action (e.g., metformin) (Kulina and Rayfield, 2016). Glucagon exerts its function via its specific receptor, the GCGR. Strategies that specifically target the GCGR, including gene knockout, antisense oligonucleotides, blocking antibodies, and peptide and non-peptide antagonists, have been developed in recent years (Lotfy et al., 2014). GCGR blockage ameliorates hyperglycemia in animal models of T1D (Conarello et al., 2007; Wang et al., 2015; Damond et al., 2016) and T2D (Sloop et al., 2004; Yan et al., 2009; Okamoto et al., 2015). Recently, the safety and efficacy of GCGR antagonists were reported in patients with T1D (Pettus et al., 2018) and T2D (Kelly et al., 2015; Kazda et al., 2016; Kazierad et al., 2016; Bergman et al., 2017; Vajda et al., 2017). However, some antagonists are accompanied by adverse events, such as hypoglycemia, increases in liver enzymes and blood pressure, and disturbed lipid metabolism, in both animal studies and clinical trials (Lotfy et al., 2014), and small-molecule antagonists (e.g., MK-0893) are particularly associated with these events (Jazayeri et al., 2016). The overall benefit-risk profiles of these antagonists do not support

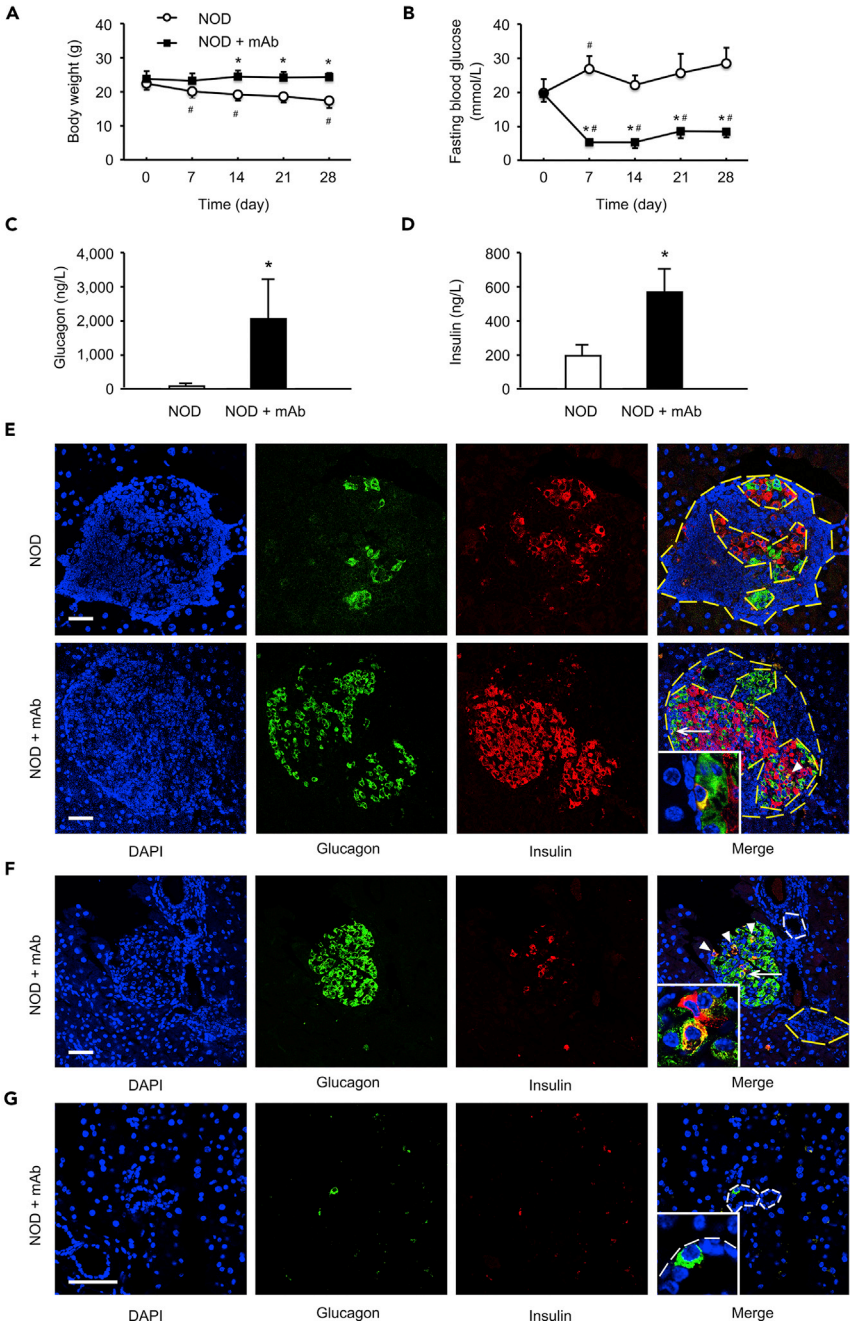

Figure 7. Metabolic Parameters and Immunofluorescence Analysis in Diabetic Female NOD Mice Treated with the GCGR mAb or Saline Control for 4 Weeks

(A–D) (A) Body weight; (B) fasting blood glucose; (C) plasma glucagon; (D) plasma insulin. n = 4–5 mice per group. Data are expressed as the mean ± S.D. Statistical analysis was conducted by Student's t test. *$p < 0.05$ (GCGR mAb vs. Saline); $^{\#}p < 0.05$ (posttreatment vs. pretreatment in the same group).

(E and F) Representative image of an islet immunostained for glucagon and insulin. The arrow and arrowheads indicate co-labeling, and the co-labeled cells indicated by the arrow are enlarged in the bottom-left corner of the image. The infiltrated lymphocytes are outlined with yellow dashed lines, and the ductal lumen is outlined with white dashed lines.

(G) Representative photograph showing glucagon-positive cells located in the ductal region in the GCGR mAb-treated NOD mice. The ductal lumen is outlined with white dashed lines. A glucagon-positive cell in the ductal lining was enlarged in the bottom-left corner of the image.

Scale bar, 100 μm. See also Figures S2C, S4B, and S7.

further clinical development (Scheen et al., 2017). Therefore, specific inhibition strategy that targets the GCGR without influencing other receptors and with minimal adverse effects is needed for clinical application. REMD 2.59, a human GCGR mAb, displays highly specific and competitive antagonistic activity against the GCGR (Yan et al., 2009), thereby minimizing potential off-target effects. This antibody shows a higher affinity to the GCGR than the cognate ligand (Yan et al., 2009), which enables it to maintain long-lasting efficacy even in hyperglucagonemia. Furthermore, this antibody has a relatively long serum half-life, thereby minimizing dosing regimens. In the present study, weekly administration of the GCGR mAb for 4 or 8 weeks had a significant hypoglycemic effect in normal, STZ-induced T1D and diabetic NOD mice. This result is in line with the data from previous studies in which the same antibody was used (Yan et al., 2009; Wang et al., 2015).

Glucagon promotes glucose production mainly via binding with the GCGR to stimulate gluconeogenesis and glycogenolysis (Quesada et al., 2008). Therefore, inhibiting the interaction between glucagon and the GCGR can improve glycemic control, primarily by reducing hepatic glucose output via inhibiting glycogenolysis (short term) and gluconeogenesis (long term) (Sloop et al., 2004; Gu et al., 2011; Lee et al., 2012). Another mechanism that may be involved in the hypoglycemic effects is the increased circulating GLP-1 level (Sloop et al., 2004; Yan et al., 2009). The findings that knocking out the *GLP-1 receptor* or the addition of its specific antagonist exendin (9–39) diminished the hypoglycemic effects of GCGR mAb treatment further support this conclusion (Gu et al., 2010). In the present study, we also found that plasma active GLP-1 was upregulated by GCGR mAb treatment in both normal and T1D mice. Innovatively, we discovered pancreatic α-cell hyperplasia, α- to β-cell conversion and, importantly, elevated plasma insulin levels in GCGR mAb-treated diabetic mice, which may represent another hypoglycemic mechanism that underlies the GCGR blockage.

In our study, treatment with the GCGR mAb boosted the pancreatic α-cell mass in both normal and T1D mice. Similarly, blocking the GCGR by gene knockout, antisense oligonucleotide, or a blocking antibody can promote α-cell neogenesis in normal mice, diet-induced obese mice, and T1D and T2D mice (Sloop et al., 2004; Lee et al., 2012; Okamoto et al., 2015). Moreover, *GCGR* mutations in human subjects have been associated with α-cell hyperplasia (Sipos et al., 2015). However, none of the studies has clarified the ontogeny of GCGR blockage-induced α-cells. We hypothesized that the expanded α-cells derived from pancreatic progenitor differentiation or pre-existing α-cell replication. In pancreatic development and organogenesis, different types of pancreatic cells bud from ducts (Freudenblum et al., 2018). Furthermore, the ducts are often recognized as the progenitor habitation and contribute to the regeneration of endocrine and acinar cells following pancreatic damage in adults (Criscimanna et al., 2011). For this reason, the location of the newly formed cells in the ducts is an indicator of cell derivation from pancreatic progenitors. In our study, most of the expanded α-cells were found in cell clusters close to ducts, some glucagon-positive α-cells were located in the ductal region, and several glucagon-positive cells were Sox9 or Hnf1β positive. These results suggest that the neogenic α-cells induced by the GCGR mAb treatment originated from the progenitor located in ducts. Besides, by cell proliferation detection, we also found that the increased α-cell mass could also result from pre-existing α-cell replication.

In addition to α-cell regeneration, the β-cell mass was boosted in the GCGR mAb-treated T1D mice. Similarly, in severe insulin-resistant mice, normalization of blood glucose with a GCGR antibody expanded the α-cell mass 5.7-fold and unexpectedly doubled the β-cell mass (Okamoto et al., 2017). These data together with our findings suggest that the GCGR antibody may promote β-cell regeneration under certain conditions. However, the specific factor that initiates this process and how the exact newborn course evolves are largely unknown. Recently, several studies have shown that pancreatic α-cells can be transdifferentiated into β-cells *in vivo* by genetic manipulation, small molecules, and currently available drugs (Collombat et al., 2009; Chung et al., 2010; Thorel et al., 2010; Al-Hasani et al., 2013; Courtney et al., 2013; Ben-Othman et al., 2017; Li et al., 2017). Based on these observations, we suspected that the newly formed β-cells induced by the GCGR mAb treatment might also have derived from α-cells. In the GCGR mAb-treated diabetic mice, we observed cells that co-expressed glucagon with insulin or other β-cell-specific markers (including Pdx1, Nkx6.1, and PC1/3), indicative of α- to β-cell conversion. Another group also found an increase in the number of a rare population of cells that co-expressed glucagon and insulin in the islets of both wild-type and *db/db* mice treated with GCGR antibody (Solloway et al., 2015). Glucagon and insulin double-positive cells might be the islet progenitor cells or the intermediary status of α- to β-cell conversion or β- to α-cell conversion. To confirm the origin of increased β-cells, we used α-cell lineage-tracing *glucagon-β-gal* mice to verify that α-cells could give birth to β-cells. As previously discussed, we noted the possibility that pancreatic progenitors located in

the ductal compartment gave rise to α-cells. Therefore, we investigated whether these neogenic β-cells could also directly derive from the progenitors. However, we did not identify insulin-positive cells in the ductal region after GCGR mAb treatment, which suggests that the progenitor cells might not directly differentiate into β-cells. In addition to derivation from α-cell reprogramming or pancreatic progenitor differentiation, the β-cell mass may increase via self-replication, but we only found a slight increase by the mAb treatment. Taken together, our results showed that treatment with the GCGR mAb promoted β-cell regeneration and the newly formed β-cells at least partially derived from α-cell conversion. Considering the importance and urgency of developing strategies with potential clinical use for diabetes therapy, the stimulating effect of GCGR mAb treatment on the β-cell mass in diabetic subjects may be a potential path for β-cell regeneration. Notably, removal of the GCGR mAb after β-cell mass increasing is a critical indicator to confirm that the β-cell mass is actually functional. Although we found that the β-cell mass in the GCGR mAb-treated diabetic mice increased after the treatment, they are far smaller than that in the normoglycemic mice. We inferred that longer duration of treatment might be needed for the mice treated with the GCGR mAb to get a significant recovery of β-cell mass.

Interestingly, we observed that the insulin staining intensity in pancreatic β-cells was weaker, and the plasma insulin level was decreased in normal C57BL/6N mice after GCGR mAb treatment. These observations could be explained by the fact that blocking GCGR signaling exerted a hypoglycemic effect; therefore, insulin production from β-cells might not be needed as much to maintain glucose homeostasis in normoglycemic mice. This finding may indicate a strategy of pancreatic β-cell rest to preserve β-cell function, similar to β-cell rest for functional recovery after intensive insulin therapy in patients with newly diagnosed T2D (Wajchenberg, 2007). Thus, treatment with the GCGR mAb might preserve β-cell function in normoglycemic mice with an ample number of β-cells and promote β-cell regeneration in T1D mice with insufficient residual β-cells, thus having different protective effects on β-cells.

As previously discussed, the GCGR mAb treatment induced α-cell hyperplasia and β-cell regeneration in T1D mice. However, the potential mechanism that underlies these results is obscure. Both glucagon and GLP-1 derive from alternative splicing of the common precursor proglucagon by PC2 and PC1/3, respectively. In mature α-cells, PC2 is the main convertase for proglucagon processing and the expression level of PC1/3 is marginal at best. In our study, GCGR mAb treatment induced PC1/3 expression in some pancreatic α-cells, thereby releasing active GLP-1 from these α-cells. This release may account for the upregulation of plasma active GLP-1 levels and the improvement of glucose homeostasis. Similarly, a previous study showed that the pancreatic preproglucagon mRNA level and pancreatic active GLP-1 content were upregulated in GCGR mAb-treated mice, and GCGR mAb-mediated improvements in glycemic control depended on functional GLP-1 receptors in pancreatic islets (Gu et al., 2010). Thus, we speculate that active GLP-1 secreted from α-cells may exert its function on adjacent pancreatic cells in a paracrine manner to promote α-cell expansion and α- to β-cell conversion. A recent study (Lee et al., 2018) reported that GLP-1 increased β-cell regeneration by promoting α- to β-cell transdifferentiation. However, adenovirus (rAd-*GLP-1*), with the risk of viral integration into the genome and carcinogenesis, was used in the study. Our study showed that GCGR mAb, a clinical potential anti-diabetic drug, had the ability to upregulate the circulating and islet local GLP-1 levels and transdifferentiate α-cells into β-cells. Considering the rapid degradation of GLP-1 by the ubiquitous dipeptidyl peptidase-4, the upregulated GLP-1 level in the islet microenvironment might play more important roles than the circulating GLP-1 in the regulation of islet cell phenotype conversion. To test this hypothesis, specific blockage of the pancreatic GLP-1 receptor will be required.

In summary, our study indicated the following: First, treatment with REMD 2.59, a human GCGR mAb, lowered the blood glucose and increased the plasma active GLP-1 levels in normal and T1D mice. Second, GCGR mAb treatment expanded the α-cell mass in normal and T1D mice and increased the β-cell mass in T1D mice. Third, the regenerated α-cells exhibited a ductal ontogeny and self-replication. Fourth, pancreatic α-cells could be converted into β-cells in GCGR mAb-treated T1D mice. Fifth, the newly formed β-cells expressed bona fide β-cell markers, suggestive of functional maturation. Our results suggest that GCGR mAb treatment may represent a promising pre-clinical strategy to improve glycemic control and restore the β-cell mass in diabetic patients.

Limitations of the Study

First, based on the location of neogenic glucagon-positive cells and the expression of the specific markers of the pancreatic progenitors detected by the immunostaining experiment, we inferred that part of the α-cells derived from the progenitor located in ducts. However, conditioned labeling for pancreatic progenitor cell activation to trace their fate is required to define the exact ductal origin of newly formed α-cells. In fact, several lineage-tracing

studies have proved that α-cells can be generated from the duct lining in adult mice (Al-Hasani et al., 2013; Courtney et al., 2013). Second, we verified that α-cells could give birth to β-cells by using *glucagon-β-gal* mice (a constitutive α-cell lineage-tracing model). However, an inducible α-cell lineage-tracing model is a more convincing tool. Third, we found the β-cell mass was enlarged by the GCGR mAb treatment. To confirm the β-cell mass is actually functional, removal of GCGR mAb after the mass increased needs be done. Forth, the potential mechanism of islet cell regeneration induced by the GCGR mAb is obscure. For instance, specific blockage of the pancreatic GLP-1 receptor will be required to determine the effects of GLP-1 in islet microenvironment. Other mechanisms including transcription factors and cytokines also needed to be investigated. Fifth, we only found islet regeneration induced by the antibody in mice and did not perform any experiments in human. Maybe human has different responses to the antibody.

METHODS

All methods can be found in the accompanying Transparent Methods supplemental file.

SUPPLEMENTAL INFORMATION

Supplemental Information can be found online at https://doi.org/10.1016/j.isci.2019.05.030.

ACKNOWLEDGMENTS

This work was supported by the National Key Research and Development Program of China (2016YFA0100501), the National Natural Science Foundation of China (81830022, 81770768, 91749101, 81570692 and 81670701), the Natural Science Foundation of Beijing (7192225), and Peking University Medicine Seed Fund for Interdisciplinary Research (BMU2018MX006).

AUTHOR CONTRIBUTIONS

R.W. and T.H. designed research; R.W., L.G., K.Y., J.L., Y.L., and S.L. performed research; H.Y. contributed new reagents; R.W., L.G., J.Y., H.W., D.T., and T.H. analyzed data; R.W. and L.G. wrote the paper; J.Y., H.Y., and T.H. revised the paper.

DECLARATION OF INTERESTS

D.T. and H.Y. are shareholders of REMD Biotherapeutics. None of the other authors has any conflicts of interest relevant to this manuscript.

Received: August 20, 2018
Revised: January 28, 2019
Accepted: May 22, 2019
Published: June 28, 2019

REFERENCES

Al-Hasani, K., Pfeifer, A., Courtney, M., Ben-Othman, N., Gjernes, E., Vieira, A., Druelle, N., Avolio, F., Ravassard, P., Leuckx, G., et al. (2013). Adult duct-lining cells can reprogram into beta-like cells able to counter repeated cycles of toxin-induced diabetes. Dev. Cell *26*, 86–100.

Ben-Othman, N., Vieira, A., Courtney, M., Record, F., Gjernes, E., Avolio, F., Hadzic, B., Druelle, N., Napolitano, T., Navarro-Sanz, S., et al. (2017). Long-term GABA administration induces alpha cell-mediated beta-like cell neogenesis. Cell *168*, 73–85.

Bergman, A., Tan, B., Somayaji, V.R., Calle, R.A., and Kazierad, D.J. (2017). A 4-week study assessing the pharmacokinetics, pharmacodynamics, safety, and tolerability of the glucagon receptor antagonist PF-06291874 administered as monotherapy in subjects with type 2 diabetes mellitus. Diabetes Res. Clin. Pract. *126*, 95–104.

Bosco, D., Armanet, M., Morel, P., Niclauss, N., Sgroi, A., Muller, Y.D., Giovannoni, L., Parnaud, G., and Berney, T. (2010). Unique arrangement of alpha- and beta-cells in human islets of Langerhans. Diabetes *59*, 1202–1210.

Bramswig, N.C., Everett, L.J., Schug, J., Dorrell, C., Liu, C., Luo, Y., Streeter, P.R., Naji, A., Grompe, M., and Kaestner, K.H. (2013). Epigenomic plasticity enables human pancreatic alpha to beta cell reprogramming. J. Clin. Invest. *123*, 1275–1284.

Brode, S., Raine, T., Zaccone, P., and Cooke, A. (2006). Cyclophosphamide-induced type-1 diabetes in the NOD mouse is associated with a reduction of CD4+CD25+Foxp3+ regulatory T cells. J. Immunol. *177*, 6603–6612.

Chung, C.H., Hao, E., Piran, R., Keinan, E., and Levine, F. (2010). Pancreatic beta-cell neogenesis by direct conversion from mature alpha-cells. Stem Cells *28*, 1630–1638.

Collombat, P., Xu, X., Ravassard, P., Sosa-Pineda, B., Dussaud, S., Billestrup, N., Madsen, O.D., Serup, P., Heimberg, H., and Mansouri, A. (2009). The ectopic expression of Pax4 in the mouse pancreas converts progenitor cells into alpha and subsequently beta cells. Cell *138*, 449–462.

Conarello, S.L., Jiang, G., Mu, J., Li, Z., Woods, J., Zycband, E., Ronan, J., Liu, F., Roy, R.S., Zhu, L., et al. (2007). Glucagon receptor knockout mice are resistant to diet-induced obesity and streptozotocin-mediated beta cell loss and hyperglycaemia. Diabetologia *50*, 142–150.

Courtney, M., Gjernes, E., Druelle, N., Ravaud, C., Vieira, A., Ben-Othman, N., Pfeifer, A., Avolio, F., Leuckx, G., Lacas-Gervais, S., et al. (2013). The inactivation of Arx in pancreatic alpha-cells triggers their neogenesis and conversion into functional beta-like cells. PLoS Genet. *9*, e1003934.

Criscimanna, A., Speicher, J.A., Houshmand, G., Shiota, C., Prasadan, K., Ji, B., Logsdon, C.D., Gittes, G.K., and Esni, F. (2011). Duct cells contribute to regeneration of endocrine and acinar cells following pancreatic damage in adult mice. Gastroenterology *141*, 1451–1462.

Damond, N., Thorel, F., Moyers, J.S., Charron, M.J., Vuguin, P.M., Powers, A.C., and Herrera, P.L. (2016). Blockade of glucagon signaling prevents or reverses diabetes onset only if residual beta-cells persist. Elife *5*, e13828.

Freudenblum, J., Iglesias, J.A., Hermann, M., Walsen, T., Wilfinger, A., Meyer, D., and Kimmel, R.A. (2018). In vivo imaging of emerging endocrine cells reveals a requirement for PI3K-regulated motility in pancreatic islet morphogenesis. Development *145*, https://doi.org/10.1242/dev.158477.

Gu, W., Lloyd, D.J., Chinookswong, N., Komorowski, R., Sivits, G., Jr., Graham, M., Winters, K.A., Yan, H., Boros, L.G., Lindberg, R.A., et al. (2011). Pharmacological targeting of glucagon and glucagon-like peptide 1 receptors has different effects on energy state and glucose homeostasis in diet-induced obese mice. J. Pharmacol. Exp. Ther. *338*, 70–81.

Gu, W., Winters, K.A., Motani, A.S., Komorowski, R., Zhang, Y., Liu, Q., Wu, X., Rulifson, I.C., Sivits, G., Jr., Graham, M., et al. (2010). Glucagon receptor antagonist-mediated improvements in glycemic control are dependent on functional pancreatic GLP-1 receptor. Am. J. Physiol. Endocrinol. Metab. *299*, E624–E632.

Jazayeri, A., Dore, A.S., Lamb, D., Krishnamurthy, H., Southall, S.M., Baig, A.H., Bortolato, A., Koglin, M., Robertson, N.J., Errey, J.C., et al. (2016). Extra-helical binding site of a glucagon receptor antagonist. Nature *533*, 274–277.

Kazda, C.M., Ding, Y., Kelly, R.P., Garhyan, P., Shi, C., Lim, C.N., Fu, H., Watson, D.E., Lewin, A.J., Landschulz, W.H., et al. (2016). Evaluation of efficacy and safety of the glucagon receptor antagonist LY2409021 in patients with type 2 diabetes: 12- and 24-week phase 2 studies. Diabetes Care *39*, 1241–1249.

Kazierad, D.J., Bergman, A., Tan, B., Erion, D.M., Somayaji, V., Lee, D.S., and Rolph, T. (2016). Effects of multiple ascending doses of the glucagon receptor antagonist PF-06291874 in patients with type 2 diabetes mellitus. Diabetes Obes. Metab. *18*, 795–802.

Kelly, R.P., Garhyan, P., Raddad, E., Fu, H., Lim, C.N., Prince, M.J., Pinaire, J.A., Loh, M.T., and Deeg, M.A. (2015). Short-term administration of the glucagon receptor antagonist LY2409021 lowers blood glucose in healthy people and in those with type 2 diabetes. Diabetes Obes. Metab. *17*, 414–422.

Kulina, G.R., and Rayfield, E.J. (2016). The role of glucagon in the pathophysiology and management of diabetes. Endocr. Pract. *22*, 612–621.

Lee, Y., Berglund, E.D., Wang, M.Y., Fu, X., Yu, X., Charron, M.J., Burgess, S.C., and Unger, R.H. (2012). Metabolic manifestations of insulin deficiency do not occur without glucagon action. Proc. Natl. Acad. Sci. U S A *109*, 14972–14976.

Lee, Y.H., Wang, M.Y., Yu, X.X., and Unger, R.H. (2016). Glucagon is the key factor in the development of diabetes. Diabetologia *59*, 1372–1375.

Lee, Y.S., Lee, C., Choung, J.S., Jung, H.S., and Jun, H.S. (2018). Glucagon-like peptide-1 increases beta cell regeneration by promoting alpha- to beta-cell transdifferentiation. Diabetes *67*, 2601–2614.

Li, J., Casteels, T., Frogne, T., Ingvorsen, C., Honore, C., Courtney, M., Huber, K.V., Schmitner, N., Kimmel, R.A., Romanov, R.A., et al. (2017). Artemisinins target GABAA receptor signaling and impair alpha cell identity. Cell *168*, 86–100.

Lotfy, M., Kalasz, H., Szalai, G., Singh, J., and Adeghate, E. (2014). Recent progress in the use of glucagon and glucagon receptor antagonists in the treatment of diabetes mellitus. Open Med. Chem. J. *8*, 28–35.

Marroqui, L., Masini, M., Merino, B., Grieco, F.A., Millard, I., Dubois, C., Quesada, I., Marchetti, P., Cnop, M., and Eizirik, D.L. (2015). Pancreatic alpha cells are resistant to metabolic stress-induced apoptosis in type 2 diabetes. EBioMedicine *2*, 378–385.

Okamoto, H., Cavino, K., Na, E., Krumm, E., Kim, S.Y., Cheng, X., Murphy, A.J., Yancopoulos, G.D., and Gromada, J. (2017). Glucagon receptor inhibition normalizes blood glucose in severe insulin-resistant mice. Proc. Natl. Acad. Sci. U S A *114*, 2753–2758.

Okamoto, H., Kim, J., Aglione, J., Lee, J., Cavino, K., Na, E., Rafique, A., Kim, J.H., Harp, J., Valenzuela, D.M., et al. (2015). Glucagon receptor blockade with a human antibody normalizes blood glucose in diabetic mice and monkeys. Endocrinology *156*, 2781–2794.

Pettus, J., Reeds, D., Cavaiola, T.S., Boeder, S., Levin, M., Tobin, G., Cava, E., Thai, D., Shi, J., Yan, H., et al. (2018). Effect of a glucagon receptor antibody (REMD-477) in type 1 diabetes: a randomized controlled trial. Diabetes Obes. Metab. *20*, 1302–1305.

Quesada, I., Tuduri, E., Ripoll, C., and Nadal, A. (2008). Physiology of the pancreatic alpha-cell and glucagon secretion: role in glucose homeostasis and diabetes. J. Endocrinol. *199*, 5–19.

Scheen, A.J., Paquot, N., and Lefebvre, P.J. (2017). Investigational glucagon receptor antagonists in Phase I and II clinical trials for diabetes. Expert Opin. Investig. Drugs *26*, 1373–1389.

Sipos, B., Sperveslage, J., Anlauf, M., Hoffmeister, M., Henopp, T., Buch, S., Hampe, J., Weber, A., Hammel, P., Couvelard, A., et al. (2015). Glucagon cell hyperplasia and neoplasia with and without glucagon receptor mutations. J. Clin. Endocrinol. Metab. *100*, E783–E788.

Sloop, K.W., Cao, J.X., Siesky, A.M., Zhang, H.Y., Bodenmiller, D.M., Cox, A.L., Jacobs, S.J., Moyers, J.S., Owens, R.A., Showalter, A.D., et al. (2004). Hepatic and glucagon-like peptide-1-mediated reversal of diabetes by glucagon receptor antisense oligonucleotide inhibitors. J. Clin. Invest. *113*, 1571–1581.

Solloway, M.J., Madjidi, A., Gu, C., Eastham-Anderson, J., Clarke, H.J., Kljavin, N., Zavala-Solorio, J., Kates, L., Friedman, B., Brauer, M., et al. (2015). Glucagon couples hepatic amino acid catabolism to mTOR-dependent regulation of alpha-cell mass. Cell Rep. *12*, 495–510.

Thorel, F., Damond, N., Chera, S., Wiederkehr, A., Thorens, B., Meda, P., Wollheim, C.B., and Herrera, P.L. (2011). Normal glucagon signaling and beta-cell function after near-total alpha-cell ablation in adult mice. Diabetes *60*, 2872–2882.

Thorel, F., Nepote, V., Avril, I., Kohno, K., Desgraz, R., Chera, S., and Herrera, P.L. (2010). Conversion of adult pancreatic alpha-cells to beta-cells after extreme beta-cell loss. Nature *464*, 1149–1154.

Unger, R.H., and Orci, L. (1977). The role of glucagon in the endogenous hyperglycemia of diabetes mellitus. Annu. Rev. Med. *28*, 119–130.

Vajda, E.G., Logan, D., Lasseter, K., Armas, D., Plotkin, D.J., Pipkin, J.D., Li, Y.X., Zhou, R., Klein, D., Wei, X., et al. (2017). Pharmacokinetics and pharmacodynamics of single and multiple doses of the glucagon receptor antagonist LGD-6972 in healthy subjects and subjects with type 2 diabetes mellitus. Diabetes Obes. Metab. *19*, 24–32.

van der Meulen, T., Lee, S., Noordeloos, E., Donaldson, C.J., Adams, M.W., Noguchi, G.M., Mawla, A.M., and Huising, M.O. (2018). Artemether does not turn alpha cells into beta cells. Cell Metab. *27*, 218–225.

Vieira, A., Courtney, M., Druelle, N., Avolio, F., Napolitano, T., Hadzic, B., Navarro-Sanz, S., Ben-Othman, N., and Collombat, P. (2016). Beta-cell replacement as a treatment for type 1 diabetes: an overview of possible cell sources and current axes of research. Diabetes Obes. Metab. *18*, 137–143.

Wajchenberg, B.L. (2007). Beta-cell failure in diabetes and preservation by clinical treatment. Endocr. Rev. *28*, 187–218.

Wang, L., Gao, P., Zhang, M., Huang, Z., Zhang, D., Deng, Q., Li, Y., Zhao, Z., Qin, X., Jin, D., et al. (2017). Prevalence and ethnic pattern of diabetes and prediabetes in China in 2013. JAMA *317*, 2515–2523.

Wang, M.Y., Yan, H., Shi, Z., Evans, M.R., Yu, X., Lee, Y., Chen, S., Williams, A., Philippe, J., Roth, M.G., et al. (2015). Glucagon receptor antibody completely suppresses type 1 diabetes phenotype without insulin by disrupting a novel diabetogenic pathway. Proc. Natl. Acad. Sci. U S A *112*, 2503–2508.

Wei, R., and Hong, T. (2016). Lineage reprogramming: a promising road for pancreatic beta cell regeneration. Trends Endocrinol. Metab. *27*, 163–176.

Yan, H., Gu, W., Yang, J., Bi, V., Shen, Y., Lee, E., Winters, K.A., Komorowski, R., Zhang, C., Patel, J.J., et al. (2009). Fully human monoclonal antibodies antagonizing the glucagon receptor improve glucose homeostasis in mice and monkeys. J. Pharmacol. Exp. Ther. *329*, 102–111.

ISCI, Volume *16*

Supplemental Information

Antagonistic Glucagon Receptor Antibody Promotes α-Cell Proliferation and Increases β-Cell Mass in Diabetic Mice

Rui Wei, Liangbiao Gu, Jin Yang, Kun Yang, Junling Liu, Yunyi Le, Shan Lang, Haining Wang, Dung Thai, Hai Yan, and Tianpei Hong

SUPPLEMENTAL FIGURES AND LEGENDS

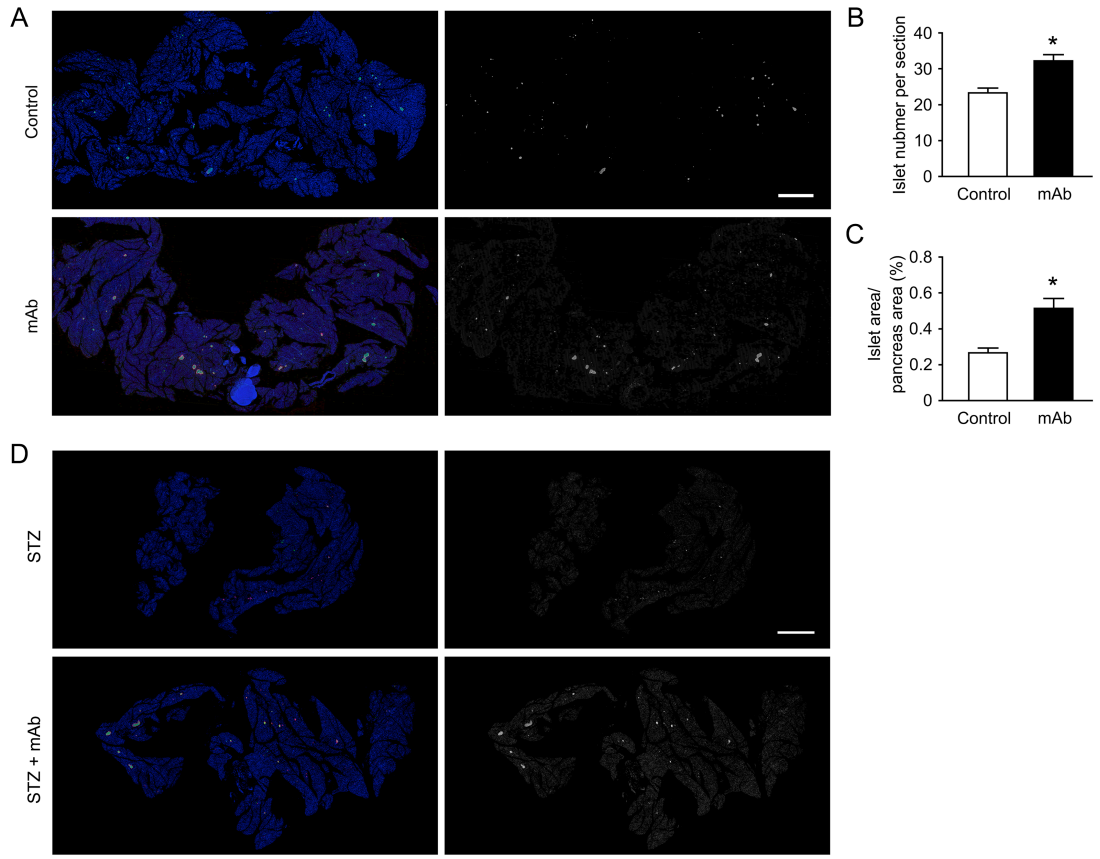

Figure S1 Related to Figures 2 and 4. Histological Analysis of the Entire Pancreata of Normal and Streptozocin (STZ)-Induced Type 1 Diabetic (T1D) Male C57BL/6N Mice Treated with REMD 2.59, a Human Glucagon Receptor (GCGR) Monoclonal Antibody (mAb) or Saline (as Control) for 4 Weeks

(A) Left panels: representative images of the whole pancreata of the normoglycemic C57BL/6N mice immunostained for glucagon (red) and C-peptide (green). Right panels: immunostaining in the same tissues as the left panels was transformed into monochrome images, and the cells immunolabeled positive for glucagon or C-peptide are displayed in white.

(B) Quantification of the islet number per pancreatic section. (C) Quantification of the islet area per pancreatic section. n = 4−6 sections/mouse multiplied by 3 mice/group. Data are expressed as the mean ± S.D. Statistical analysis was conducted by Student's t test. *$p < 0.05$ (GCGR mAb vs. control).

(D) Left panels: representative images of the whole pancreata of the STZ diabetic mice immunostained for glucagon (red) and C-peptide (green). Right panels: immunostaining in the same tissues as the left panels was transformed into monochrome images, and the cells immunolabeled positive for glucagon or C-peptide are displayed in white.

Scale bar, 2000 μm.

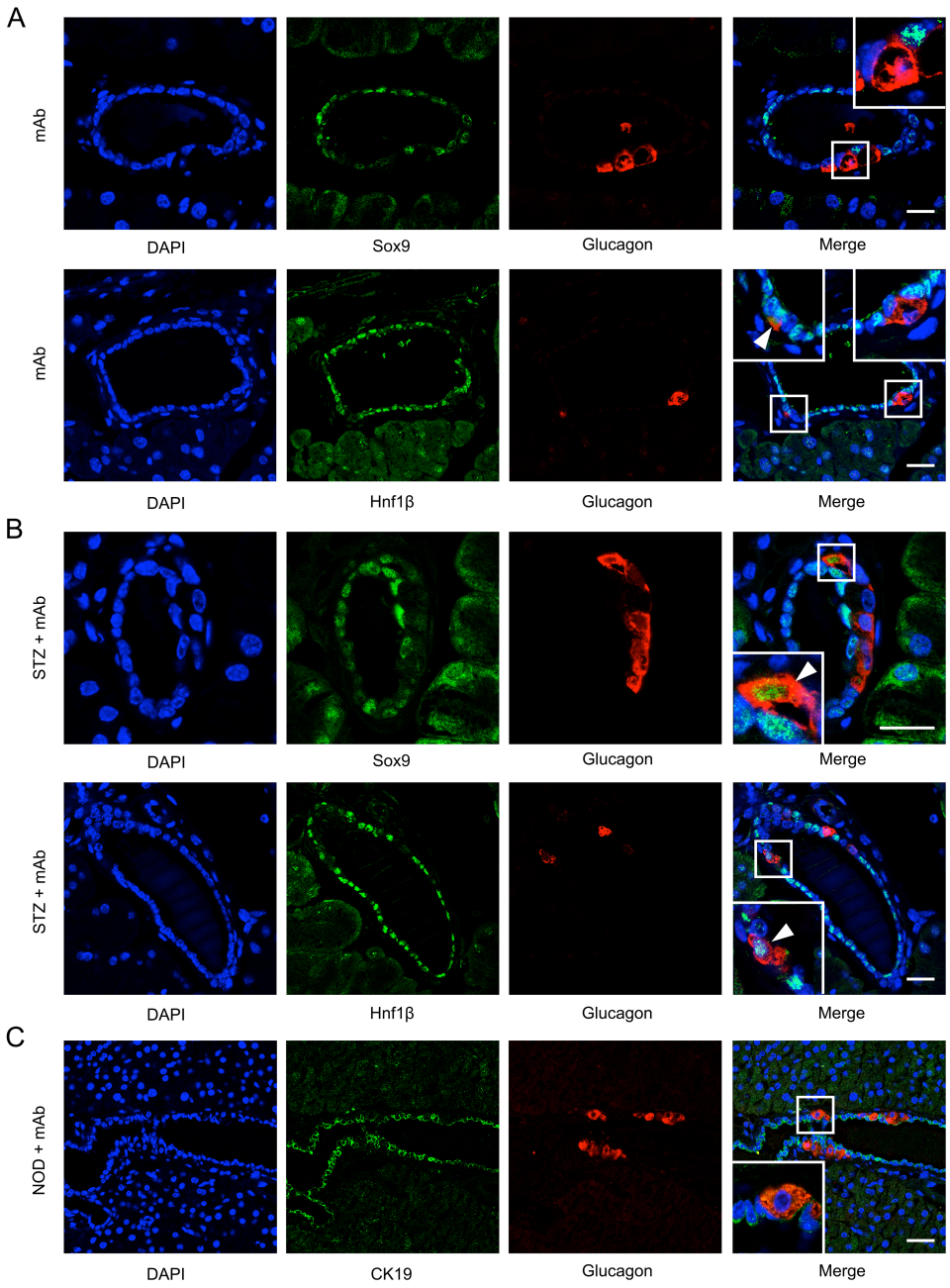

Figure S2 Related to Figures 2, 4 and 7. Histological Analysis in the Pancreata of Normal (A) and STZ-Induced T1D (B) Male C57BL/6N Mice, and Diabetic Female NOD Mice (C) Treated with the GCGR mAb or Saline Control for 4 Weeks

(A-B) Representative images of co-labeling for the duct cell marker Sox9 (upper lanes) or Hnf1β (lower lanes) with glucagon.

(C) Representative images of co-labeling for the mature duct cell marker cytokeratin 19 (CK19) with glucagon.

The cells in the small box are enlarged at the corners of the images. Glucagon-positive cells were located in the ductal region or co-localized with duct cells (indicated by the arrowheads). Scale bar, 50 μm.

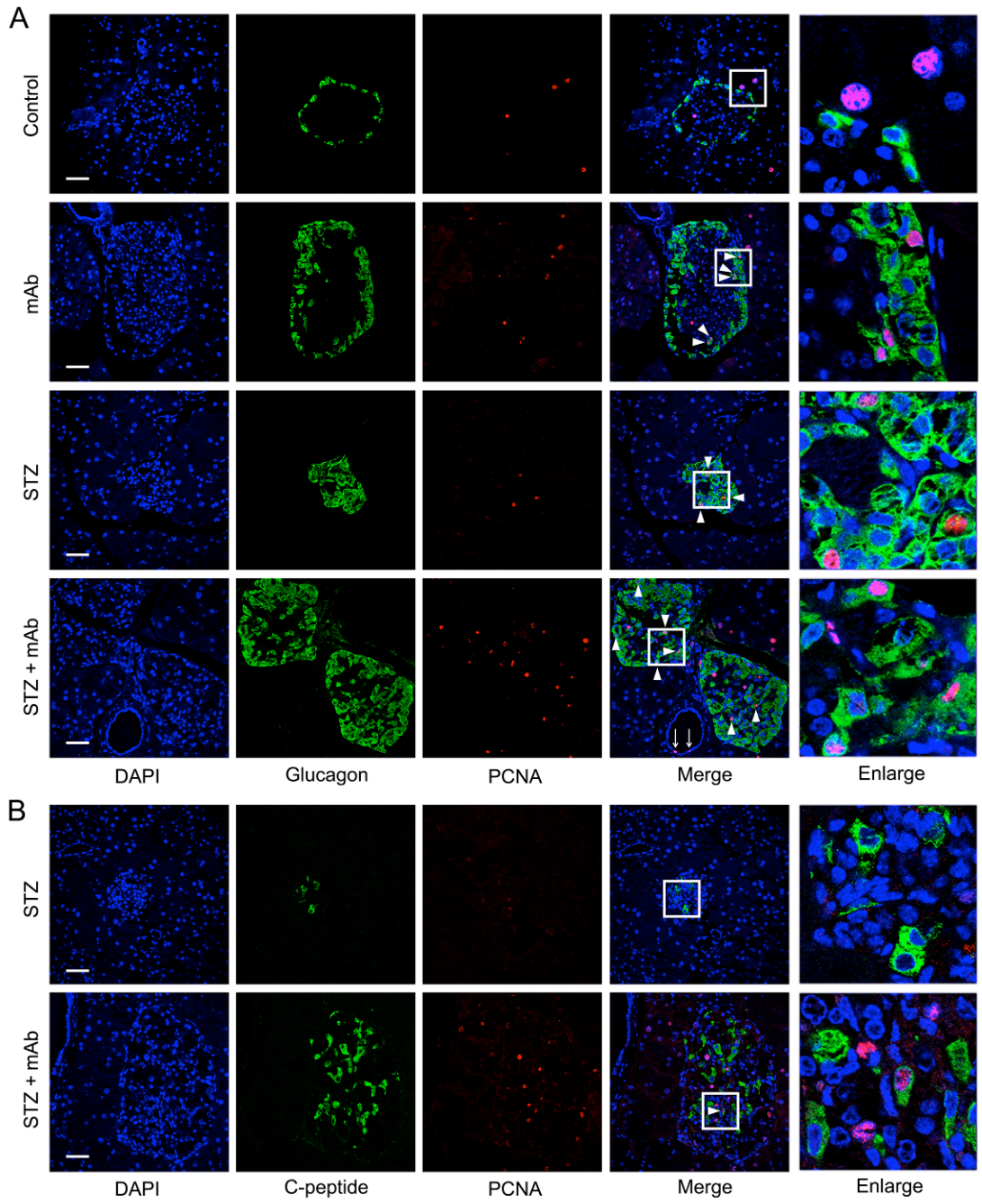

Figure S3 Related to Figures 2 and 4. Histological Analysis in the Pancreata of Normal and STZ-Induced T1D Male C57BL/6N Mice Treated with the GCGR mAb or Saline Control for 4 Weeks

(A) Representative images of co-labeling for glucagon with PCNA, a proliferating marker.

(B) Representative images of co-labeling for C-peptide with PCNA.

The double-labeling cells are indicated by the arrowheads. The PCNA positive cells in the ductal region are indicated by the arrow. The cells in the small box are enlarged in the fifth columns. Scale bar, 100 μm.

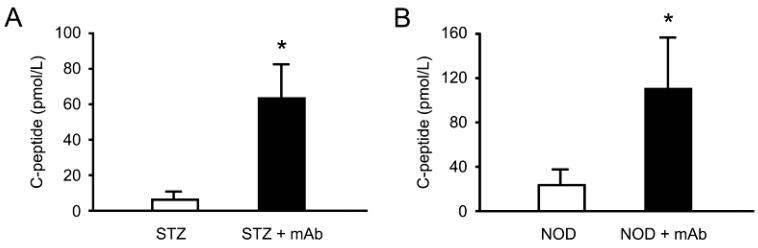

Figure S4 Related to Figures 3 and 7. Plasma C-peptide in the STZ-Induced T1D Mice (A) and Diabetic NOD Mice (B) Treated with the GCGR mAb or Saline Control for 4 Weeks

Data are expressed as the mean ± S.D. Statistical analysis was conducted by Student's t test. *$p < 0.05$.

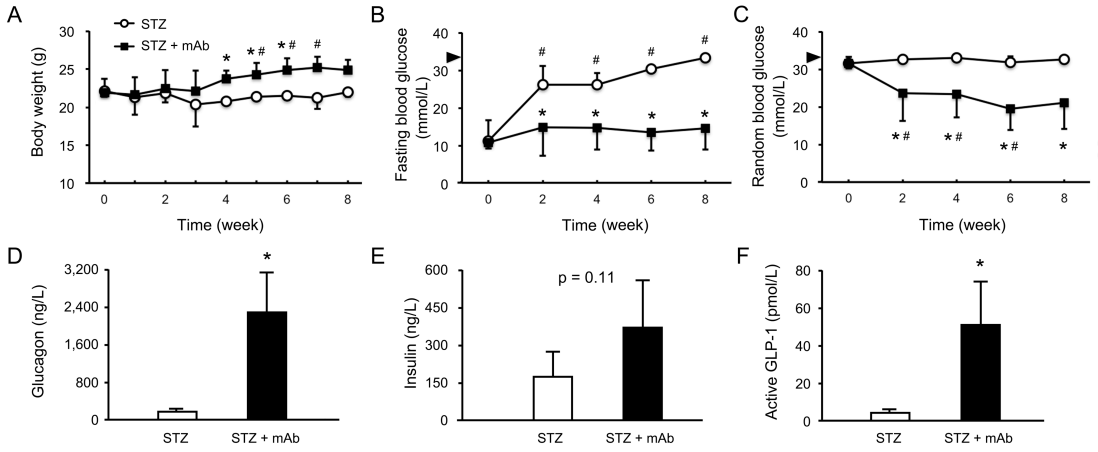

Figure S5 Related to Figure 5. Metabolic Parameters in STZ-Induced T1D Male *Glucagon-β-gal* Mice Treated with the GCGR mAb or Saline Control for 8 Weeks

(A) Body weight; (B) fasting blood glucose; (C) random blood glucose; (D) plasma glucagon; (E) plasma insulin; (F) plasma active glucagon-like peptide-1 (GLP-1). n = 5 mice per group. Data are expressed as the mean ± S.D. Statistical analysis was conducted by Student's t test. *$p < 0.05$ (GCGR mAb vs. Saline); $^{\#}p < 0.05$ (post-treatment vs. pretreatment in the same group). The arrowheads in (B and C) indicate the upper detection limit of the glucometer (33.3 mmol/L).

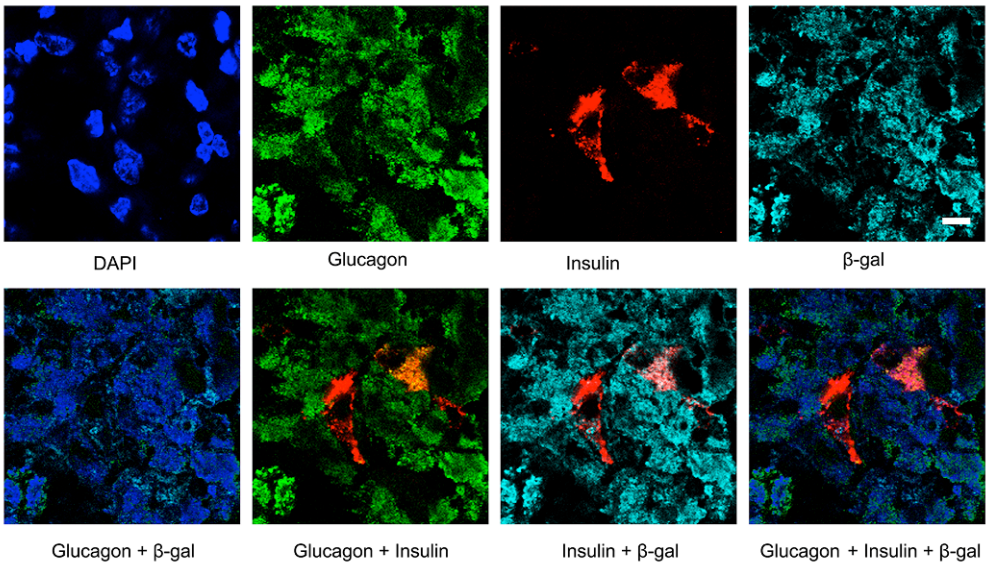

Figure S6 Related to Figure 5. Immunofluorescence Analysis of Co-labeling for Glucagon, Insulin and β-gal in STZ-induced T1D *Glucagon-β-gal* Mice Treated with the GCGR mAb for 8 Weeks

Representative image of an islet immunostained with glucagon, insulin and β-gal. Scale bar, 10 μm.

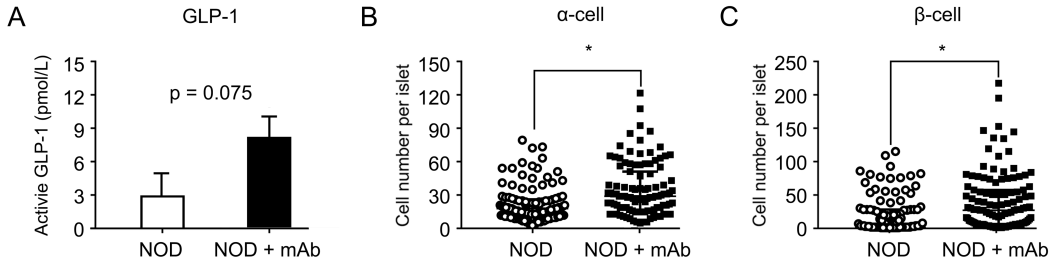

Figure S7 Related to Figure 7. Plasma Active GLP-1 Level and Immunofluorescence Quantification of the Pancreata in the Diabetic NOD Mice Treated with the GCGR mAb or Saline Control for 4 Weeks

(A) Plasma active GLP-1 level in the NOD mice. n = 5 mice per group. Data are expressed as the mean ± S.D. Statistical analysis was conducted by Student's t test. *p < 0.05 (GCGR mAb vs. Saline).

(B-C) Quantification of α- and β- cells per islet slice. n = 6 sections/mouse multiplied by 4 mice/group. Data are expressed as the median (interquartile range). Statistical analysis was conducted by the Mann-Whitney test. *p < 0.05 (GCGR mAb vs. Saline).

TRANSPARENT METHODS

Animals, Intervention and Monitoring

All animal experiments were conducted at Peking University Health Science Center (Beijing, China) and were approved by the Institutional Animal Care and Use Committee. Eight-week-old male C57BL/6N mice were group-housed conventionally and maintained on a 12-h light/dark cycle with free access to food and water. The animals were treated for 4 weeks via intraperitoneal administration of REMD 2.59 (5 mg/kg), a human GCGR mAb and competitive antagonist, or saline (5 ml/kg, as control) once per week.

To establish a T1D model, 150 mg/kg STZ in citric acid buffer (0.1 mol/L, pH 4.2) was administered into male C57BL/6N mice via intraperitoneal injection. One to two weeks after STZ injection, the diabetic condition was confirmed if the fasting blood glucose was ≥ 11.1 mmol/L or the random blood glucose was ≥ 16.7 mmol/L. The diabetic mice were single-housed to improve survival and treated for 4 weeks via intraperitoneal administration of REMD 2.59 (5 mg/kg) or saline once per week.

B6.Cg-Tg(Gcg-cre)1Herr/Mmnc (cre expression in pancreatic α-cell lineage) and B6;129-Gt(ROSA)26Sor^{tm1Sho}/J (when crossed to a cre recombinase-expressing strain, lacZ expression is observed in the cre-expressing tissues) mice were crossed to generate pancreatic α-cell lineage-tracing mice, namely, *glucagon-β-gal* mice. Eight-week-old male *glucagon-β-gal* mice were induced into a diabetic model by 150 mg/kg STZ as previously described, and the diabetic mice were then single-housed

and treated for 8 weeks via weekly injection of REMD 2.59 (5 mg/kg) or saline.

Forty female NOD mice were group-housed for the onset of diabetes. At week 18, 11/40 mice were diabetic with a fasting blood glucose ≥ 11.1 mmol/L. Ten mice were treated via weekly injection of REMD 2.59 (5 mg/kg) or saline for 4 weeks.

For all experiments, the mice were randomly assigned to different groups to ensure an unbiased distribution. There were 5-10 mice per group. During the study period, the body weight and blood glucose were monitored every week.

Glucose Measurement

All blood samples were collected from tails, and glucose was measured by the glucose oxidase method using a hand-held OneTouch Ultra glucometer (LifeScan, Milpitas, CA). For the measurement of fasting blood glucose, the normal mice were fasted 15 h, and the diabetic mice were fasted 8 h. Random blood glucose levels were measured at 9:00 a.m. If the glucose level was greater than 33.3 mmol/L (upper detection limit of the glucometer), the value of 33.3 mmol/L was recorded.

Assays of Plasma Hormones

Blood samples for hormone detection were collected from the orbital vein. A dipeptidyl peptidase-4 inhibitor (50 μmol/L), aprotinin (1 μg/mL) and heparin sodium (1000 IU/mL) were added to each blood sample. The plasma glucagon, insulin, C-peptide, and active GLP-1 were detected by ELISA.

Immunofluorescence Staining

Pancreata were fixed with 10% (*v*/*v*) neutral-buffered formalin at 4 °C overnight and embedded in paraffin, and 5-μm-thick sections were prepared. For immunofluorescence, the sections were heated in an autoclave in a citrate buffer (12 mmol/L, pH 6.0), pre-incubated in a permeabilization blocking buffer (0.1 mmol/L PBS, pH 7.3, 0.5% Triton) and blocked for 30 min with 10% (*v*/*v*) goat serum (Zhongshan Biotechnology, Beijing, China). The cells were subsequently incubated with primary antibodies at 4 °C overnight and secondary antibodies for 1 h at room temperature, followed by washing and staining with DAPI (1 μg/mL). Images were captured under a confocal fluorescence microscope (Zeiss LSM710, Carl Zeiss Microscopy GmbH, Jena, Germany) or an automatic digital slide scanner (Pannoramic MIDI, 3D HISTECH, Budapest, Hungary). Negative controls were performed using the corresponding isotypic sera instead of the primary antibodies.

Quantification of Immunostaining

For cell quantification in the immunofluorescence staining, 5 to 10 equally spaced sections per pancreas were imaged, and the total numbers of positive staining cells from at least 3 mice per group were counted manually or using Image-Pro Plus 6.0. Approximately 200 cells in the T1D mice without GCGR mAb treatment and 500 cells in the diabetic mice treated with the GCGR mAb and normal C57BL/6N mice were counted.

Statistical Analysis

Data are expressed as the mean ± S.D. or median (interquartile range). Differences between two groups were analyzed using Student's t test (two-tailed) or the Mann-Whitney test, as appropriate. A p value < 0.05 was considered statistically significant. Statistical analysis was performed using GraphPad Prism 7.0.

KEY RESOURCES TABLE

REAGENT or RESOURCE	SOURCE	IDENTIFIER
Antibodies		
Rabbit polyclonal anti-glucagon (1:800)	Cell Signaling Technology	Cat#2760; RRID: AB_659831
Mouse monoclonal anti-glucagon (1:400)	Sigma-Aldrich	Cat#G2654; RRID: AB_259852
Mouse monoclonal anti-insulin (1:800)	Sigma-Aldrich	Cat#I2018; RRID: AB_260137
Rabbit polyclonal anti-C-peptide (1:400)	Cell Signaling Technology	Cat#4593; RRID: AB_10691857
Rabbit monoclonal anti-CK19 (1:400)	Abcam	Cat#ab52625; RRID: AB_2281020
Rabbit polyclonal anti-Sox9 (1:100)	Millipore	Cat#AB5535; RRID: AB_2239761
Rabbit polyclonal anti-Hnf1β (1:50)	Santa Cruz	Cat#sc22840
Mouse monoclonal anti-PCNA (1:400)	Cell Signaling Technology	Cat#2586
Rabbit polyclonal anti-Pdx1 (1:200)	Abcam	Cat#ab47267; RRID: AB_777179
Rabbit monoclonal anti-Nkx6.1 (1:400)	Abcam	Cat#ab221549; RRID: AB_2754979
Rabbit polyclonal anti-PC1/3 (1:400)	Millipore	Cat#AB10553; RRID: AB_1977441
Chick anti-β-galactosidase (1:100)	Abcam	Cat#ab9361
Alexa Fluor 594-conjugated AffiniPure goat polyclonal anti-mouse IgG (H+L) (1:800)	Jackson ImmunoResearch Laboratories	Cat#115-585-003; RRID: AB_2338871
Alexa Fluor 488-conjugated AffiniPure goat polyclonal anti-rabbit IgG (H+L) (1:800)	Jackson ImmunoResearch Laboratories	Cat#111-545-003; RRID: AB_2338046
Alexa Fluor 647-conjugated AffiniPure donkey polyclonal anti-chicken IgG (H+L) (1:400)	Jackson ImmunoResearch Laboratories	Cat#703-605-155
Chemicals, Peptides, and Recombinant Proteins		
Streptozocin (STZ)	Sigma-Aldrich	Cat#S0130
REMD 2.59 (a human GCGR mAb and competitive antagonist)	REMD Biotherapeutics	N/A
Dipeptidyl peptidase-4 inhibitor	Millipore	Cat#DPP4
Aprotinin	Sigma-Aldrich	Cat#ROAPRO
DAPI	Sigma-Aldrich	Cat#D9542

Critical Commercial Assays		
Glucagon ELISA kit	R&D Systems	Cat#DGCG0
Insulin ELISA kit	Millipore	Cat#EZRMI-13K
C-peptide ELISA kit	Millipore	Cat#EZRMCP2-21K
Active GLP-1 ELISA kit	Millipore	Cat#EGLP-35K
Experimental Models: Organisms/Strains		
Mouse: C57BL/6N	Vital River Animal Center, Beijing, China	Cat#213
Mouse: B6.Cg-Tg(Gcg-cre)1Herr/Mmnc	Mutant Mouse Resource & Research Centers supported by NIH (MMRRC)	Cat# 000358-UNC; RRID: MMRRC_000358-UNC
Mouse: B6;129-Gt(ROSA)26Sor^{tm1Sho}/J	The Jackson Laboratory	Cat#003504
Mouse: NOD/ShiLtJNju	Nanjing Biomedical Research Institute of Nanjing University, China	Cat#N000235
Software and Algorithms		
Image-Pro Plus 6.0	Media Cybernetics	N/A
GraphPad Prism 7.0	GraphPad Software Inc.	N/A